https://doi.org/10.5194/bg-2021-50
Preprint. Discussion started: 9 March 2021


Biogeosciences Discussions
Open Access
EGU

# An analysis of the macroalgal $\delta^{13}C$ variability in the Gulf of California

Roberto Velázquez-Ochoa[a], María Julia Ochoa-Izaguirre[b], Martín F. Soto-Jiménez[c*]

[a]Posgrado en Ciencias del Mar y Limnología, Universidad Nacional Autónoma de México, Unidad Académica Mazatlán, Mazatlán, Sinaloa 82040, México

[b]Facultad de Ciencias del Mar, Universidad Autónoma de Sinaloa. Paseo Claussen s/n, Mazatlán, Sinaloa 82000, México

[c]Unidad Académica Mazatlán, Instituto de Ciencias del Mar y Limnología, Universidad Nacional Autónoma de México (UAM-ICMyL-UNAM), Mazatlán Sinaloa, 82040, México.

Correspondent author:

Telephone number: +52 (669) 9852845 to 48.

Fax number: +52 (669) 9826133

E-mail: martin@ola.icmyl.unam.mx

https://doi.org/10.5194/bg-2021-50
Preprint. Discussion started: 9 March 2021


Biogeosciences Discussions Open Access EGU

17 **Abstract**

18 The C isotopic composition in macroalgae ($\delta^{13}C$) is highly variable, and its prediction is very
19 complex relative to terrestrial plants. To contribute to the knowledge on the variations and
20 determinants of $\delta^{13}C$-macroalgal, we analyzed a large stock of specimens varying in taxa and
21 morphology and inhabiting shallow marine habitats from the Gulf of California (GC)
22 featured by distinctive environmental conditions. A large $\delta^{13}C$ variability (-34.61‰ to -
23 2.19‰) was observed, mostly explained on the life form (taxonomy, morphology, and
24 structural organization), and modulated by the interaction between habitat features and
25 environmental conditions. The intertidal zone specimens had less negative $\delta^{13}C$ values than
26 in the subtidal zone. Except for pH, environmental conditions of the seawater do not
27 contribute to the $\delta^{13}C$ variability. Specimens of the same taxa showed $\delta^{13}C$ similar patterns,
28 to increase or decrease, with latitude (21º-30°N). $\delta^{13}C$-macroalgal provides information on
29 the inorganic carbon source used for photosynthesis ($CO_2$ diffusive entry vs $HCO_3^-$ active
30 uptake). Most species showed a $\delta^{13}C$ belong into a range that indicates a mix of $CO_2$ and
31 $HCO_3^-$ uptake; the $HCO_3^-$ uptake by active transport is widespread among GC macroalgae.
32 About 20-34% of species showed the presence of carbon concentrating mechanism (CCM).
33 Ochrophyta presented a high number of species with $\delta^{13}C$>-10‰, suggesting widespread
34 $HCO_3^-$ use by non-diffusive mechanisms. Few species belonging to Rhodophyta relied on
35 $CO_2$ diffusive entry ($\delta^{13}C$<-30‰) exclusively. $\delta^{13}C$ provides useful information about the
36 physiological and environmental status of macroalgae.

37 **Keywords:** $\delta^{13}C$-macroalgal, carbon-concentrating mechanisms, $CO_2$ diffusive proxy

38

39

https://doi.org/10.5194/bg-2021-50
Preprint. Discussion started: 9 March 2021


Biogeosciences Discussions Open Access EGU

## 1. Introduction

Macroalgae shows a wide diversity of morphologies, structural organization (e.g., surface area/volume ratio), and various pigments. Based on these features, macroalgae can be classified into only three phyla, in agreement to the pigment contents in the thallus, or in dozens of groups considering morphologies and pigments (Littler and Littler, 1980; Littler & Arnold, 1982; Balata et al., 2011). For example, mixing of chlorophyll (*a*, *b*) and carotenoids are usually observed in Chlorophyta; chlorophyll (*a*, *c*) is dominant in Ocrophyta. Rhodophyta contains chlorophyll (*a*, *d*), carotenoid, and a mix of phycobilin (e.g., phycocyanin, phycoerythrina, allophycocyanin) (Bold and Wynne, 1978; Masojidek et al., 2004; Gateau et al., 2017). Both traits work as an excellent approximation to explain the fundamentals of metabolism, growth, zonation, and colonization (Littler and Littler, 1980; Littler and Arnold, 1982; Nielsen and Sand-Jensen, 1990; Vásquez-Elizondo and Enríquez, 2017).

Thallus thickness as the propriety of the morphology influences the diffusion boundary layer at the macroalgal surface, where the uptake of essential ions and dissolved gases by macroalgae occur (Hurd, 2000; San-Ford and Crawford, 2000). In marine environments, where pH~8.1±1, $HCO_3^-$ accounting 98% of total DIC due to the low diffusion rate of $CO_2$ in seawater that results in a high $HCO_3^-$ : $CO_2$ ratio (150:1) (Sand-Jensen and Gordon, 1984). The limitations for growth imposed by low seawater $CO_2$ concentrations are compensated by carbon concentrating mechanisms (CCMs) in most of macroalgae that increase internal carbon inorganic concentration (near the site of RuBisCo activity (Giordano et al., 2005). For hence, $HCO_3^-$ uptake by most macroalgae is the principal inorganic carbon source for photosynthesis, but a few species depend exclusively on to use of dissolved $CO_2$ that enter by diffusion to the cells (Maberly et al., 1992; Beardall and Giordano, 2002; Raven et al.,

https://doi.org/10.5194/bg-2021-50
Preprint. Discussion started: 9 March 2021


64 2002a, b; Giordano et al., 2005). So, macroalgal species with productivity limited by lacking
65 CCM's (have low plasticity for carbon inorganic forms uptake) seems to be restricted to
66 submareal habitats and composed mainly by red macroalgae (but without a morphological
67 patron apparent) (Cornwall et al., 2015, Kübler and Dungeon, 2015). The rest of the
68 macroalgae with CCM occupies from the intertidal to the deep submareal.
69 Nevertheless, marine ecosystems have many environmental factors, including habitat
70 features and environmental conditions in seawater that modify the main macroalgae
71 photosynthesis drivers (light, DIC, and inorganic nutrients). These factors could generate
72 negative consequences for their productivity, principally when they cause resources
73 limitation. Each factor varies from habitat to habitat (e.g., local scale: from intertidal to
74 subtidal and global scale: from temperate to tropical regions), and as in response to these
75 environmental changes, macroalgae can modulate their photosynthetic mechanism (Lapointe
76 and Duke, 1984; Dudgeon et al., 1990; Kübler and Davison 1993, Young et al., 2005). The
77 modulation, to increase their photosynthetic activity (up-and-down-regulation processes),
78 implies a physiological acclimation enhancing the transport of DIC ($CO_2$, $HCO_3^-$) into the
79 cell and its fixation rates (Madsen and Maberly, 2003; Klenell et al., 2004; Zou et al., 2004;
80 Giordano et al., 2005; Enríquez and Rodriguez-Román, 2006; Rautemberger et al., 2015).
81 The $\delta^{13}C$ on the thallus of marine macrophytes is a proxy used to identify $CO_2$ or $HCO_3^-$
82 source in photosynthesis and to infer the presence or absence of CCM's (Maberly et al., 1992;
83 Raven et al., 2002a). Also, the $\delta^{13}C$ signal in the algal thallus can be used as an indicator of
84 the physiological state of photosynthetic metabolism (Kim et al., 2014; Kübler and Dungeon,
85 2015). Consequently, $\delta^{13}C$ variability depends, in part, on the life form (taxonomy,
86 morphology, and structural organization), but also is modulated by the interaction to

https://doi.org/10.5194/bg-2021-50
Preprint. Discussion started: 9 March 2021


environmental conditions (light, DIC, and nutrients). Thus, the prediction of the $\delta^{13}C$ variability in marine macrophytes is very complex relative to terrestrial plants.

In this study, our objective was to investigate the contributions of life form, the changes in the habitat features, and environmental conditions to the $\delta^{13}C$ macroalgal variability in communities in the Gulf of California (GC). A second objective was to describe the proportion of species that lacks CCM inferred by the δ13C signal along and between the GCE bioregions. A third objective was to explore any geographical pattern in the $\delta^{13}C$ macroalgal. Macroalgae as biomonitor constitute an efficient tool in monitoring programs in large geographical regions (Balata et al., 2011) and for environmental impact assessments (Ochoa-Izaguirre and Soto-Jiménez, 2014).

To reach our objectives, we collected a large stock of macroalgae specimens of a diversity of species characterized by a variety of morphological and physiological properties. Besides high diversity, in terms of life forms, we selected various shallow marine habitats along a latitudinal gradient in the GCE for the sample collection, characterized by unique and changing environmental factors. The GCE features abundant and diverse macroalgae populations, which are acclimated and adapted to diverse habitats with environmental conditions, determining the light, DIC, and nutrients availability.

## 2. Materials and Methods

### 2.1. Gulf of California description

The Gulf of California is a subtropical, semi-enclosed sea of the Pacific coast of Mexico, with exceptionally high productivity being the most important fishing regions for Mexico and one of the most biologically diverse worldwide marine areas (Zeitzschel, 1969; Espinosa-Carreón and Valdez-Holguín 2007; Lluch-Cota et al., 2007; Páez-Osuna et al., 2017). GC represents only

https://doi.org/10.5194/bg-2021-50
Preprint. Discussion started: 9 March 2021


109 0.008% of the area covered by the seas of the planet (265,894 km$^2$, 150 km wide, and 1000 km
110 long covering >9 degrees latitude) but has a high physiographic diversity and is biologically mega-
111 diverse with many species endemic (Wilkinson et al., 2009; Espinosa-Carreón and Escobedo-
112 Urías, 2017).

113 Regionalization criteria of the GC include phytoplankton distribution (Gilbert and Allen, 1943),
114 topography (Rusnak et al., 1964) and depth (Álvarez-Borrego, 1983), oceanographic characteristics
115 (Roden and Emilson, 1979; Álvarez-Borrego, 1983; Marinone, 2003), biogeography (Santamaría-
116 del-Ángel et al., 1994a), and bio-optical characteristics (Bastidas-Salamanca et al., 2014). The
117 topography is variable along GC, includes submarine canyons, basins, and variable continental
118 platform. Besides, GC presents complex hydrodynamic processes, including internal waves, fronts,
119 upwelling, vortices, mixing of tides. The gulf's coastline is divided into three shores: extensive
120 rocky shores, long sandy beaches, numerous scattered estuaries, coastal lagoons, and open muddy
121 bays tidal flats and coastal wetlands (Lluch-Cota et al., 2007).

122 The Gulf of California is different in the north and the south, related to a wide range of
123 physicochemical factors. The surface currents seasonally change direction and flow to the
124 Southeast with maximum intensity during the winter and to the Northwest in summer (Roden
125 (1958). The northern part is very shallow (<200 m deep averaged), divided into Upper Gulf,
126 Northern Gulf, and Grandes Islas. The surrounding desserts largely influence this region (Norris,
127 2010) shows marked seasonal changes in coastal seawater temperatures (Martínez-Díaz de León et
128 al., 2006; Marinone, 2007). Tidal currents induce a significant cyclonic circulation through June to
129 September and anticyclonic from November to April (Carrillo et al., 2002; Bray, 1988a; Velasco-
130 Fuentes and Marinone, 1999; Martínez-Díaz-de-León, 2001). The southern part consists of a series
131 of basins whose depths increase towards the South (Fig. 1). The intertidal macroalgae in the

https://doi.org/10.5194/bg-2021-50
Preprint. Discussion started: 9 March 2021


132 southern region are subject to desiccation, mostly during summer. The water column's
133 physicochemical characteristics are highly influenced by the contrasting climatic seasons in the
134 GC, the dry season (nominally from November to May), and the rainy season (from June to
135 October). Annual precipitation (1,080 mm $y^{-1}$) and evaporation (56 mm $y^{-1}$) rates registered during
136 the past 40 years were 881±365 mm $y^{-1}$ and 53±7 mm $y^{-1}$, respectively (CNA, 2012).

137 Previous macroalgae floristic studies of the CG, report around 580 species, including 116 endemic
138 species (Norris, 1975; Espinoza-Avalos, 1993). Based on oceanographic characteristics (Roden and
139 Groves, 1959) and in the endemic species distribution (Aguilar Rosas and Aguilar Rosas, 1993), the
140 CGE can be classified into three phycofloristic zones: 1) First zone located from the imaginary line
141 connecting San Francisquito Bay, B.C. to Guaymas, Sonora, with 51 endemic species. 2) the Second
142 zone with an imaginary line from La Paz bay (B.C.S.) to Topolobampo (Sinaloa) with 41 endemic
143 species. 3) the Third zone is located with an imaginary line from Cabo San Lucas (B.C.S.) to Cabo
144 Corrientes (Jalisco) with 10 endemic species. Besides, 14 endemic species are distributed throughout
145 the GCE (Espinoza-Ávalos, 1993). The macroalgal communities are subject to the changing
146 environmental conditions in the diverse habitats in the GCE that delimits their zonation, which
147 tolerates a series of anatomical and physiological adaptations to water movement, temperature, sun
148 exposure, and light intensities, low pCO2, desiccation (Espinoza-Avalos 1993).

149 **2.1 Macroalgae sampling**

150 In this study, the GC coastline (21°-30°N latitude) was divided into six coastal sectors based on the
151 three phycofloristic zones previously described (Fig. 1a). In each selected ecosystem, representative
152 habitats were sampled based on macroalgae communities' presence and habitat characterization.
153 Habitats were classified by substrate type (e.g., sandy-rock, rocky shore), hydrodynamic (slow to

https://doi.org/10.5194/bg-2021-50
Preprint. Discussion started: 9 March 2021


faster water flows), protection level (exposed or protected sites), and immersion level (intertidal or subtidal) (Fig. 1b).

Based on the local environmental factors, macroalgae specimens (4-5) of the most representative species were gathered by hand (free diving) during low tide. A total of 809 composite samples were collected from marine habitats along both G.C. coastlines. The percentages of specimens collected for the substrate type were sandy-rock 28% and rocky shores 72% based on the habitat features. Related to the hydrodynamic, 30% of the specimens were collected in habitats with slow to moderate and 70% with moderate to fast water movement. Regarding the protection level, 57% were exposed specimens, and 43% were protected. Finally, 56% were intertidal and 44% subtidal macroalgae organisms concerning the emersion level. About half of the protected specimens were collected in isolated rock pools, which was noted.

In 4-5 sites of each habitat, we measured *in situ* the salinity, temperature, and pH by using a calibrated multiparameter sonde (Y.S.I. 6600V) and the habitat characteristics mentioned above noted. Besides, composite water samples were collected for nutrient and alkalinity in the laboratory. Briefly, the representative habitats were classified by pH levels in >9.0 “alkalinized”, 7.9-8.2 ‘typical’ and <7.9 “acidified”. Based on the temperature in colder <20ºC, typical 20-25ºC, and warmer >25ºC. 72% of the specimens were collected at typical pH values, 22% in alkalinized and 6% in acidified seawater. Regarding the temperature, about 55% of the specimens were collected at typical, 31% at warmer, and 14% at colder seawaters. Regarding salinity, most of the ecosystems showed typical values for seawater (35.4±0.91 ups, from 34.5 to 36.1 ups). In this study, the collection surveys were conducted during spring (March-April) and dry season (nominally from November to May) from 2009 to 2014. Only in few selected ecosystems located at C1 and C2 sectors, one sampling survey was conducted at the end of the rainy season (nominally from June to October

https://doi.org/10.5194/bg-2021-50
Preprint. Discussion started: 9 March 2021


in 2014). Thus, these ecosystems were possible to include habitat with a salinity range varying from estuarine (23.5±3.0 ups) to hypersaline (42.7±7.0 ups) values. These habitats were mainly isolated rockpools, and only a few were sites near tidal channels receiving freshwater discharges. About 95% of the specimens were collected at typical seawater salinity and only 1.5 and 3.5% in estuarine and hypersaline environments. Detailed information on the selected shallow marine ecosystems, habitat characterization, and environmental conditions is summarized in the inserted table in Fig. 1.

### 2.2 Macroalgae processing and analysis of the isotopic composition of carbon

The collected material was washed *in situ* with surface seawater to remove the visible epiphytic organisms, sediments, sand, and debris and then thoroughly rinsed with MilliQ water. The composite samples were double-packed in a plastic bag, labeled with the locality's name and collection date, placed in an ice-cooler box to be kept to 4ºC, and immediately transported to the laboratory UAS-Facimar in Mazatlán. In the field, sample aliquots were also preserved in 4% v/v formaldehyde solution for taxonomic identification to the genus or species level (when possible). The following GC macroalgal flora identification manuals were consulted: Dawson, 1944; 1954; 1956; 1961; 1962; 1963; Setchell and Gardner, 1920; 1924; Abbott and Hollenberg, 1976; Ochoa-Izaguirre et al., 2007; Norris, 2010).

In the laboratory, macroalgae samples were immediately frozen at -30ºC until analysis. Then, samples freeze-dried at -38ºC and 40 mm Hg for 3 days, upon which they were ground to a fine powder and exposed to HCl vapor for 4 h (acid-fuming) to remove carbonates and dried at 60ºC for 6 h (Harris et al. 2001). Five milligrams aliquots were encapsulated in tin cups (5x9 mm) and stored in sample trays until analysis. Macroalgae samples were sent to the Stable Isotope Facility (SIF) at the University of California at Davis, CA, USA. Natural $^{13}C$ relative abundance relative to

https://doi.org/10.5194/bg-2021-50
Preprint. Discussion started: 9 March 2021


$^{12}C$ in samples was determined with mass spectrometry, using a Carlo Erba elemental analyzer attached to a Finnigan Delta S mass spectrometer equipped with a Europa Scientific stable isotope analyzer (ANCA-NT 20-20) and a liquid/solid preparation unit (PDZ, Europa, Crewz, UK). Isotope ratios of the samples were calculated using the equation $\delta$ (‰)=($R_{sample}/R_{standard}$-1)]x1000, where R=$^{13}C/^{12}C$. The $R_{standard}$ is relative to the international V-PDB (Vienna PeeDee Belemnite) standard. During the isotopic analysis, the SIF lab used different certified reference materials (e.g., IAEA-600, USGS-40, USGS-41, USGS-42, USGS-43, USGS-61, USGS-64, an USGS-65) for the analytical control quality. The analytical uncertainties reported for the SIF lab were 0.2‰ for $\delta^{13}C$ (https://stableisotopefacility.ucdavis.edu/13cand15n.html). We also included triplicate aliquots of several specimens of the same species and condition, collected from one patch or attached to the same substrate, to assess the method error by sampling and processing procedural. The methodological uncertainties were <0.4‰.

### 2.3. Analysis of $\delta^{13}C$-macroalgal variability

The variability of $\delta^{13}C$ values in macroalgae was analyzed in function of the taxonomy (phylum, genus, and species) and morpho-functional groups (e.g., thallus structure, growth form, branching pattern, and taxonomic affinities; Balata et al. 2011; Ochoa-Izaguirre and Soto-Jiménez, 2015).

Sampled specimens belong to three phyla, 63 genera, and 167 species. The phyla were identified as Rhodophyta (53%), Ochrophyta (22%) and Chlorophyta (25%). The most representative genus (and their species) were Ulva (*U. lactuca, U. lobata, U. flexuosa,* and *U. intestinalis*), Codium (*C. amplivesiculatum* and *C. simulans*), Chaetomorpha (*C. antenina*), Padina (*P. durvillaei*), Dictyota (*D. dichotoma*), Colpomenia (*C. tuberculata* and *C. sinuosa*), Sargassum (*S. sinicola* and *S. horridum*), Amphiroa (*Amphiroa* spp.), *Spyridia* spp, *Polysiphonia* spp., *Gymnogongrus* spp.,

https://doi.org/10.5194/bg-2021-50
Preprint. Discussion started: 9 March 2021


Gracilaria (*G. vermiculophylla*, *G. pacifica* and *G. crispate*), Hypnea (*H. pannosa* and *H. johnstonii*) Grateloupia (*G. filicina* and *G. versicolor*), and Laurencia (*L. papillosa* and *L. pacifica*). An analysis of the biogeographical diversity among sectors evidenced that P3 (43 genera of 63, 68%) and C3 (63%) at north recorded the highest number of genus, followed by C1 (38%) and P1 (29%) at the south, and P2 (27%) and C2 (22%). The same pattern was observed in the species richness, zones P3 (94 of 167 species, 56%) and C3 (52%) at the north, C1 (34%) and P1 (25%) at south, and C2 and P2 (19-20%) at the center.

In order to find a geographic pattern associated with the $\delta^{13}C$ signal of macroalgae in this study, macroalgae were grouped according to their characteristics morpho-functional proposed initially by Littler and Littler (1980) and modified by Balata et al. (2011). Not all morphofunctional groups and taxon were present in every site during each sampling survey, and the sample size in each group varied for taxa, location, and time. The morphofunctional groups identified were 21, of which the most common were C-tubular (6 spp., n=69; C-Blade-like (6 spp, n=55); C-Filamentous uniseriate (17 spp, n=49); C-Erect thallus (5 spp, n=33); O-Compressed with branched or divided thallus (19 spp., n=92); O-Thick leathery macrophytes (12 spp., n=104); O-Hollow with spherical or subspherical shape (4spp, n=87); R-Large-sized corticated (57 spp., n=225); R-Filamentous uniseriate and pluriseriate with erect thallus (9 spp., n=48); and R-Large-sized articulated corallines (6 spp, n=17). The diversity, in terms of presence/absence of the morphofunctional groups, varied among coastline sectors, higher in C3 (16 of 21, 76%) and P3 (71%) at the north, followed by C1 (57%) and P1 (48%) at the south, and C2 and P2 and (42-48%) at the center of both GC coastlines. Detailed information on macroalgae specimens collected (ecosystem, habitat, number of composite samples, morphological group, and taxon) is given as Supplementary Information (Table SI-1).

A basic statistical analysis of $\delta^{13}C$ values in different macroalgae groups was applied to distribute

https://doi.org/10.5194/bg-2021-50
Preprint. Discussion started: 9 March 2021


and calculate the arithmetic mean, standard deviation, minimum and maximum. Because not all macroalgal species were present in sufficient numbers at different collection habitats, several macroalgal groups were not considered for statistical analysis. Regarding the life form, we compared among morphofunctional groups, taxon collected in the same habitat (within-subjects factor) by multivariate analysis of variance. When differences were noted, a Tukey-Kramer HSD (Honestly Significant Difference) test was performed. Besides, variations of $\delta^{13}C$ macroalgal in specimens of the same morpho-functional and taxon collected in different habitats were also investigated with a Kruskal-Wallis test.

In this study, the relationships between $\delta^{13}C$ with each independent variable related to the inherent macroalgae properties (morphology and taxon), biogeographical collection zone (GC coastline and coastal sector), habitat features (substrate, hydrodynamic, protection, and emersion level) and environmental conditions (temperature, pH, and salinity) were examined through simple and multiple linear regression analyses. Excepting temperature, pH, and salinity, most of the independent variables are categorical independent variables. However, these continue variables were also categorized, such as previously was described. Analyses of simple linear regression were performed to establish the relationships between $\delta^{13}C$-macroalgal with each environmental parameter analyzed as possible driving factors (e.g., temperature, salinity, pH). Multiple linear regression analyses were conducted to evaluate the combined effects of those independent variables (macroalgae properties, biogeographical collection zone, habitat features, and environmental conditions) on the $\delta^{13}C$-macroalgal. In the multivariable regression model, the dependent variable, $\delta^{13}C$-macroalgal, is described as a linear function of the independent variables $X_i$, as follows: $\delta^{13}C\text{-macroalgal} = a + b_1(X_1) + b_2(X_2) + \ldots + b_n(X_n)$ (1). Where a is regression constant (it is the value of intercept and its value is zero); $b_1$, $b_2$, and $b_n$, are regression coefficients for each independent variable $X_i$. From each

https://doi.org/10.5194/bg-2021-50
Preprint. Discussion started: 9 March 2021


one of the fitted regression models, we extracted the estimated regression coefficients for each of the predictor variables (e.g., Bayesian Information Criterion (BIC), Akaike Information Criterion (AIC), root-mean-square error (RMSE), Mallow's Cp criterion, F Ratio test, p-value for the test (Prob > F), coefficients of determination ($R^2$) and the adjusted $R^2$ statistics) (SAS Institute Inc., 2018). All regression coefficients were used as indicators of the quality of the regression (Draper and Smith, 1998; Burnham and Anderson, 2002). Kolmogorov-Simirnov normality test was applied for all variables and all were normally distributed. Most of the $\delta^{13}C$ values in each group showed a normal distribution. For all statistical tests, a probability $P<0.05$ was used to determine statistical significance. The statistical analysis of the results was done using JMP 14.0 software (SAS Institute Inc.).

## 3. Results

### 3.1. $\delta^{13}C$-macroalgal variability in function of taxonomy and morpho-functional groups

The variability of $\delta^{13}C$ values in macroalgae was analyzed by taxon in the phylum, genus, species, and morphofunctional groups. Ochrophyta displayed the values from -21.5 to -2.20‰ (-12.55±3.77‰), significantly higher to Chlorophyta (-25.92 to -5.57‰, -14.55±3.04‰) and Rhodophyta (-34.61 to -4.55‰, -14.84±3.96‰) (Fig. 2a-c). The $\delta^{13}C$-macroalgal values (average±SD) for the genus of Chlorophyta, Ochrophyta, and Rhodophyta (Fig. 2d-f) varied from -33.79±1.17‰ for *Schizymenia* to -7.86±0.73‰ for *Amphiroa*. Multiple comparisons among the genera more representative of each taxon showed the following order *Schizymenia* < *Polysiphonia* < *Ulva*, *Gracilaria* and *Spyridia* (-16.17±0.67‰ to -15.11±0.26‰) < *Gymnogongrus*, *Laurencia*, *Hypnea*, *Cladophora*, *Dictyota*, *Sargasumm*, *Chaetomorpha*, and *Grateloupia* (from -15.40±0.71‰

https://doi.org/10.5194/bg-2021-50
Preprint. Discussion started: 9 March 2021


289 to -13.86±0.78‰) < *Codium* and *Padina* (-12.52±2.46‰ to -12.45±2.54‰) < *Colpomenia* and
290 *Amphiroa* (-9.26±0.32 to -7.86±0.73‰). Aggrupation of $\delta^{13}C$ values based on morpho-functional
291 features on macroalgae id displayed in Fig. 3. The most representative groups in the phylum
292 Chlorophyta varied from -15.83±0.37‰ for C-Tubular to -12.45±0.54‰ for C-thallus erect. The
293 phylum Ochrophyta includes O-Thick leathery with the lowest mean (-14.79±0.30‰) and O-Hollow
294 with a spherical or subspherical shape with the highest values (-9.26±0.33‰). The lowest and highest
295 $\delta^{13}C$ values for Rhodophyta were observed for R-flattened macrophytes (-24.0±9.63‰) and for R-
296 Larger-sized articulated coralline (-7.89±0.75‰), respectively. Significant differences were
297 observed among groups, which were ordered as follows: R-flattened macrophytes<R-blade like < C-
298 Tubular < O-Tick leathery and R-Large size corticated < C-Blade like and C-Filamentous uniseriate
299 < C-Erect thallus and O-Compressed with branch < O-Hollow with spherical < R-Larger-sized
300 articulated coralline.

301 By multiple comparison analysis of the same genus at different coastal sectors (Fig. 4), non-
302 significant differences were observed among coastal sectors for most of the genus, except for
303 *Amphiroa*, *Codium*, *Padina*, and *Spyridia* with $\delta^{13}C$ values systematically more negatives in
304 continental than peninsular coastline (C1-C3 > P1-P3). Also, lower $\delta^{13}C$ values were observed in the
305 C2 sector for most of the genus and higher at P1 and P3. Due to the strong influence of genera
306 composition on the morphofunctional group, similar results were found, and the graph is no showed.

307 For the most representative species, a detailed comparative analysis of macroalgal $\delta^{13}C$ values was
308 also conducted and displayed on Table 1-3 for phyla Chlorophyta, Ochrophyta, and Rhodophyta,
309 respectively. For *Codium*, *C. brandegeei* (11.82±1.24‰) and *C. simulans* (-11.43±2.20‰) showed
310 higher $\delta^{13}C$ values than *C. amplivesculatum* (-14.44±2.74‰). The three *Colpomenia* species had
311 higher $\delta^{13}C$ values than the other genera. *C. tuberculata* (-8.75±3.2‰) showed values significantly

https://doi.org/10.5194/bg-2021-50
Preprint. Discussion started: 9 March 2021


higher than *Colpomenia* sp. (-10.97±3.65‰) and *C. sinuosa* (-10.18±2.95‰). The four-representative species of *Gracilaria* showed comparable $\delta^{13}C$ values, averaging from -16.48±1.64‰ for *G. pacifica* to -15.48±2.43‰ for *Gracilaria* sp. Three representative species of *Hypnea* showed non-significant $\delta^{13}C$ differences, varied from -16.4±1.75‰ for *H. spinella* to -14.95±2.36‰ for *Hypnea* sp. two species represented Laurencia, *Laurencia* sp. (-12.90±1.22‰) higher than *L. pacifica* (-14.9±2.20‰). Two species represented *Padina*, being *Padina* sp. (-11.10±1.53‰) higher than *P. durvillaei* (-13.20±2.59‰). *Sargassum* was one of the most diverse genera studied with six representative species. Based on the $\delta^{13}C$ values the species were ordered as follow: *S. horridum* = *S. sinicola* = *S. johnstoniis* (-15.52±2.89 to -15.10±2.41‰) < *S. lapazeanum* (-14.49±1.59‰) = *Sargassum* sp. (-14.25±2.36‰) < *S. herphorizum* (-13.65±1.63‰). *Spyridia* was represented by *Spyridia* sp. (-17.06±1.20‰) and *S. filamentosa* (-15.86±3.83‰) without significant differences. The six representative species of *Ulva* were divided in two morphological groups, filamentous and laminates. Filamentous species that averaged -16.35±2.01‰ for *U. clathrata*, -16.03±3.64‰ for *U. flexuosa*, -15.78±1.72‰ for *U. acanthophora* and -15.29±2.54‰ for *U. intestinalis* and Ulva laminates that included *U. linza* (-15.56±2.44‰) and *U. lactuca* (-14.10±3.13‰). Non-significant differences were observed between morphological groups and among species. A high intra-specific variability, 11-28%, explains average overlapping.

### 3.2. Taxonomy versus habitat features

Variability of $\delta^{13}C$ values for the most representative genera was evaluated by multiple comparative analyses in the habitat features' function, including the substrate, hydrodynamic, and emersion level. Large $\delta^{13}C$ variability observed between specimens of the same genus collected in the different habits does not show any significant pattern, and non-significant differences were observed. An exception was observed with the emersion level (showed in Fig. 5), where intertidal specimens

https://doi.org/10.5194/bg-2021-50
Preprint. Discussion started: 9 March 2021


recorded less negative values than subtidal in most macroalgae genus. For example, for *Hydroclathrus* (intertidal -5.74±0.89‰; subtidal -11.46±5.93‰), *Amphiroa* (Intertidal -6.93±1.52; Subtidal -9.91±6.14), *Hypnea* (intertidal -13.56±2.56‰; submareal -18.60±1.88‰), and *Laurencia* (intertidal -13.49±1.36‰; subtidal -17.11±1.80‰). Exceptions were observed for *Polysiphonia* (intertidal -19.74±2.27‰, subtidal -14.94±6.69‰), *Spyridia* (intertidal -16.97±3.33‰, subtidal -13.21±0.73‰) and *Colpomenia* (Intertidal -9.41±3.41‰, subtidal -7.76±1.34‰).

### 3.3. Taxonomy versus environmental conditions

Non-significant differences were observed for the same genera at different temperatures ranges, except for *Grateloupia* (cold, -19.28±4.70‰, typical -14.45±2.23‰, warm -14.57±2.25‰) and *Polysiphonia* (cold, -21.05±0.46‰, typical -18.12±5.54‰, warm -17.96±2.38‰) with more negative values in colder than warmer waters. Significant differences were observed in $\delta^{13}C$ values in macroalgae specimens from the different genus in the same temperature range. For example, *Colpomenia* (cold -8.34±2.43‰, typical -9.47±3.77‰, warm -9.22±2.64‰), *Codium* (cold -11.98±1.91‰, typical -12.54±3.01‰, warm -13.61±0.62‰), and *Padina* (cold -11.34±2.55‰, typical -11.88±1.76‰, warm -13.42±2.77‰) (Fig. 6a), was less negative than the other genus.

Overall, more negative $\delta^{13}C$ values in macroalgae specimens' values of the same genus were observed at continental (C2) compared to peninsular CG coastline (P1-P3) and more negative southward than northward.

Significant differences were observed among genus related to the pH level at seawater (Fig. 6b). Typical pH seawater, *Amphiroa* (-8.80±5.44) and *Colpomenia* (-10.29±3.66‰) were 1-2‰ more negatives than in alkaline waters, while *Ulva* (-15.08±2.47‰) and *Spyridia* (-15.34±2.12‰) were 3-5‰ less negative than in acidic waters. *Amphiroa* and *Colpomenia* were not collected in acidic water,

https://doi.org/10.5194/bg-2021-50
Preprint. Discussion started: 9 March 2021


357 and neither *Spyridia* in alkaline waters to compare. Another genus also showed extremes values
358 between alkaline (*Tacanoosca* -7.60±1.01‰) and acidic waters (*Schizymenia*, -32.96±2.01‰). The
359 following order was observed in the genus collect at the three pH ranges: alkaline > typical > acidic.
360 Significant differences were observed for genus *Ahnfeltiopsis*, *Caulerpa*, *Gymnogongrus*, *Padina*,
361 and *Ulva*, with higher values at alkaline than in acidic waters. Values of $\delta^{13}C$ for specimens of the
362 same genus collected at typical pH waters are mostly overlapped between those for alkaline and
363 acidic seawaters. Non-significant differences in $\delta^{13}C$ values were observed for *Grateloupia*, *Hypnea*,
364 and *Polysiphonia* concerning pH-type waters.

365 Regarding the $\delta^{13}C$ variability for all data set in response to temperature and salinity, a non-
366 significant trend was observed between $\delta^{13}C$-macroalgal in both parameters' function. A poor
367 bivariate correlation, but significant, was observed between $\delta^{13}C$ with pH ($R^2 = 0.04$) (Fig. 7).

368 **3.4. Variation latitudinal of $\delta^{13}C$-macroalgal**

369 The $\delta^{13}C$-macroalgal variation in the GC biogeography was evaluated by regression linear analysis
370 between $\delta^{13}C$ values along the nine degrees latitude in both GC coastlines. A non-significant
371 latitudinal trend was observed for datasets, but for the three taxa's most representative genera, $\delta^{13}C$
372 values correlated with latitude (Fig. 8a-f). In Chlorophyta, with the higher genera number, $\delta^{13}C$
373 values increased with latitude (Fig. 8a) with a weak but significant correlation. Contrarily, in
374 Ochrophyta (Fig. 8b) and Rhodophyta (Fig. 8c) specimens, the $\delta^{13}C$ values decreased with latitude.

375 Significant correlations ($p<0.001$) were observed for $\delta^{13}C$-macroalgal *versus* latitude in the most
376 representative morphofunctional groups. Representative morphofunctional groups of Chlorophyta
377 (e.g., C-Tubular, C-Filamentous uniseriate, Fig. 8d) showed a positive correlation, while those
378 belonging to Ochrophyta (e.g., O-thick leathery; Fig. 8e) and Rhodophyta (e.g., R-large sized

https://doi.org/10.5194/bg-2021-50
Preprint. Discussion started: 9 March 2021


379 corticated.; Fig. 8f) showed a negative trend with latitude.

380 **3.5. Analyses of $\delta^{13}C$ macroalgal variability**

381 An analysis of the effects, independent and combined, on the $\delta^{13}C$-macroalgal variability
382 related to life form and environmental factors was conducted. Firstly, simple linear regression
383 analyses were performed to evaluate the dependent variable's prediction power ($\delta^{13}C$-
384 macroalgal) in the function of several independent variables controlling the main macroalgae
385 photosynthesis drivers (light, DIC, and inorganic nutrients). Regression coefficients were
386 estimated for each fitted regression model, which are used as indicators of the quality of the
387 regression (Draper and Smith, 1998; Burnham and Anderson, 2002) as was described in
388 Methods; however, our results description focused on the coefficients of determination ($R^2$ and
389 adjusted $R^2$). The coefficient $R^2$ describes the overall relationship between the independent
390 variables $X_i$ with the dependent variable Y ($\delta^{13}C$-macroalgal), and it is interpreted as the % of
391 contribution to the $\delta^{13}C$ variability. While the adjusted $R^2$ statistics compensate for possible
392 confounding effects between variables.
393 Results of the analysis of the relationships between $\delta^{13}C$ with each independent variable are
394 summarized in Table 4. Regarding the inherent macroalgae properties, Phyla explain only
395 7% variability, the morphofunctional properties 35%, and taxon by genus 46%, and by
396 species 57%. The biogeographical collection zone, in terms of coastline (continental vs.
397 peninsular) and coastal sectors (C1-C3 and P1-P3), explained a maximum 5% variability.
398 Related to the habitat features, only emersion level (6%) contributed to the $\delta^{13}C$ variability.
399 The contribution of the seawater's environmental conditions was marginal for pH (4%) and
400 negligible for temperature and salinity. A marginal reduction in the percentage of

https://doi.org/10.5194/bg-2021-50
Preprint. Discussion started: 9 March 2021


401 contribution was observed for Phyla (1%) and morphofunctional properties (1%), but
402 significant for genus (5%) and species (10%).
403 Multiple regression analyses were also performed to interpret the complex relationships
404 among $\delta^{13}$C-macroalgal, considering the life form (morphofunctional and taxon by genus)
405 and their responses to environmental parameters. Results for the fitted regression models
406 performed for morphofunctional groups (Table 5) and genus (Table 6) evidenced that the
407 effect of the coastal sector and pH ranges on the $\delta^{13}$C-macroalgal increased the contribution
408 by 9-10% each one. The emersion level increased by 5-6%, the contribution respect to
409 individual effect of morphofunctional group and genus, the temperature and pH in 1 and 3%,
410 respectively, while salinity decreased by 1-2%. Adding the effect of the biogeographical
411 collection zone, represented by the coastline sector, to those for morphofunctional group
412 (Table 5) and genus (Table 7), a notable increase of 11-12% was observed.
413 The full model considering the combined effect of the coastline sector + Habitats features for
414 Morphofunctional group or Genus (Table 7), showed $R^2$ of 0.60 and 0.71. In contrast,
415 Coastline sector + Environmental conditions + Morphofunctional group or Genus the $R^2$
416 increased to 0.62 and 0.72, respectively. The interactive explanations of environmental
417 factors increased the explanation percentage of $\delta^{13}$C variability; however, these contributions
418 were significantly lower than the explained by life forms, such as the morphofunctional
419 properties and taxa by genus and species.
420 The combined effect of environmental condition on the $\delta^{13}$C variability was tested for the best-
421 represented morphological groups and genus. Results evidenced that 9 of 21 morphological groups
422 showed significant effects on the $\delta^{13}$C variability (Table 8), five increasing and four decreasing the
423 model constant of $\delta^{13}$C=-14.21‰. For example, for the O-Hollow with spherical or subspherical
424 shape (+4.96‰) and R-Larger-sized articulated corallines (+6.32‰) the predicted values are -

https://doi.org/10.5194/bg-2021-50
Preprint. Discussion started: 9 March 2021


425 7.89±0.80‰ and -9.25±0.47‰. For R-Filamentous uniseriate and pluriseriate with erect thallus (-
426 2.15‰) and C-Tubular (-1.62‰) the predicted values are -16.36±0.55‰ and -15.83±0.50‰,
427 respectively. Regarding taxon, a significant effect was observed only in 13 genera, including
428 *Colpomenia* (+5.45‰), *Amphiroa* (+6.84‰), and *Padina* (+2.19‰) increasing the signal, and
429 *Polysiphonia* (-3.75‰), *Gracilaria* (-0.89‰), and Spyridia (-1.46‰) decreasing the signal of the
430 model constant (Table 9). In 33 species was observed a significant effect on the $\delta^{13}C$ variability,
431 including *C. tuberculate* +5.87‰, *C. sinuosa* +4.42‰, *H. pannosa* +4.42‰, *H. johnstonii* +4.42‰,
432 and *Amphiroa spp*. (+4.42 to 8.20‰) increasing the model constant $\delta^{13}C$= -14.59‰, and *Spyridia*
433 sp. (-2.46‰), *G. filicina* (-2.37‰), *P. mollis* (-5.22‰) and *S. pacifica* (-19.19‰) (Table 9).
434

435 **4. Discussions**

436 **4.1. Relationship among taxonomy and habitat with $\delta^{13}C$ signal**

437 Our analyses showed high variability in the $\delta^{13}C$ signal in the large inventory of macroalgae collected
438 along GC coastline for five years. Most authors studying the isotopic composition of C in these
439 organisms have reported the high isotopic variability, which has been attributable to the taxon-
440 specific photosynthetic Ci acquisition properties (Raven et al., 2002, Mercado et al., 2009, Marconi
441 et al., 2011, Stepien, 2015). Following the mechanistic explanation of $\delta^{13}C$ signal for algal thallus,
442 values of $\delta^{13}C$ more negative than -30‰ indicate that photosynthesis is exclusively dependent on
443 $CO_2$ diffusion (absence of CCM), whereas values above -10‰ indicate non-diffusive Ci transport
444 mechanism ($HCO_3^-$ users by the presence of CCM; Maberly et al., 1992; Raven et al., 2002). To
445 explain our results, no considerate of the $CO_2$ leak out inside the cell could occur and change the
446 cutoffs for $CO_2$ or $HCO_3^-$ users (Sharkey and Berry, 1985; Raven et al., 2005).

https://doi.org/10.5194/bg-2021-50
Preprint. Discussion started: 9 March 2021


447 In our study, 84% of the analyzed specimens belong into the intermediate range between -30‰ and
448 -10‰, averaging -14.05±3.98‰, which is slightly higher than the global mean for intertidal
449 macroalgal -17.35±0.43‰ based on the meta-analysis of macroalgal $\delta^{13}C$ compiled by Stepien
450 (2015). The apparent differences in the $\delta^{13}C$ averages can be related to the organism origin, mostly
451 from temperate and polar marine ecosystems (142 sampling sites temperate, eight sites from tropics,
452 and six from polar zones) in the Stepien (2015) compilation concerning the subtropical marine
453 ecosystems in our study. Our global mean includes the specimens collected at submareal and
454 intertidal habitats because non-significant differences were observed in most macroalgae groups.

455 These results suggest that macroalgal communities from subtropical marine ecosystems record
456 higher values than communities from temperate. Seawater from temperate zones has more $CO_2$
457 dissolved availability, which results in more negative carbon isotopic values in macroalgae when the
458 Ci is incorporated into the tissue (Raven et al., 2002ab). $\delta^{13}C$ values evidence that most of the
459 sampled macroalgae in our study have an active CCM to fix involves the direct use of $HCO_3^-$ with
460 little $CO_2$ diffusive uptake (Giordano et al., 2005; Hopkinson et al., 2011; Hopkinson, 2014; Raven
461 and Beardall, 2016). However, based only on the $\delta^{13}C$ values, it is not possible to discern that CCM
462 type is expressing in the organisms (e.g., direct $HCO_3^-$ uptake by the anion-exchange protein AE;
463 Drechsler and Beer 1991; Drechsler et al. 1993). However, it is possible to assume that at least one
464 basal carbon concentrating mechanism (bCCM) is active. The most primitive mechanism is the $CO_2$
465 diffusion (Cerling et al., 1993) that could be composed of two types of mitochondrial carbonic
466 anhydrase (e.g., internal and external) that enhance the fixation of Ci by recycling mitochondrial
467 $CO_2$ (Zabaleta et al., 2012). The role of carbonic anhydrase (CA) in algal photosynthesis was
468 described since the end-1960s (Bowes, 1969) and more recently detailed by Jensen et al. (2020),
469 who described the CA types and their functions. Also, the co-existence of different CCM's have

https://doi.org/10.5194/bg-2021-50
Preprint. Discussion started: 9 March 2021


470 been described for the same species (Axelsson et al., 1999, Xu et al., 2012), even that different
471 CCM's can operate simultaneously, generating different Ci contribution to RuBisCo internal pool
472 (Rautemberger et al., 2015). The variety of CCMs and their combinations contribute to the high $\delta^{13}C$
473 variability for the same species.

474 Because the carbon isotopic discrimination decreases when photosynthesis rates increase (Kübler
475 and Dungeon, 2015), less negative values in GC macroalgae could evidence higher productivity in
476 subtropical seaweed communities than those in temperate marine ecosystems. A high $\delta^{13}C$ on
477 macroalgae tissue require saturating light intensity and enough nutrients availability (Dudley et al.,
478 2010), conditions occurring in the GC waters. Based on the plant communities' pattern, G.C.'s
479 macroalgal community productivity with intermediates values (so-called hump-back) belonging to
480 intermediate productivity (Grime, 1970; Pärtel et al., 2007; Pärtel and Zobel, 2007).

481 On the other hand, species that high efficiently $HCO_3^-$ uptake, according to their $\delta^{13}C$ signal, were
482 to 35 (20%, >-10‰). Alternatively, 58 species (34%) of 170 species, if -11.5‰ (Δ of 1.5‰ as
483 respiratory effect) is the cutoff value for $HCO_3^-$ users according to Carvalho and Eyre (2011). About
484 20-34% of species could have the biochemical machinery to fix directly $HCO_3^-$, an efficient CCM
485 that potencies the productivity when is growing under optimal conditions. Furthermore, the highest
486 δ13C values have been associated with the intermediate C3-C4 or C4 pathway (Valiela et al., 2018),
487 which suggests a more efficient C.C.M.'s than the typical C3 pathway. The C4 pathway reduces
488 photorespiration, the antagonist process of RuBisCo that causes a reduction in Ci assimilation about
489 25-40% (Ehleringer et al., 1991; Bauwe et al., 2010; Zabaleta et al., 2012). C4 pathway plants'
490 photorespiration reduction could be explained by their resource allocation, where they have more
491 investment in C.C.M. than in RuBisCo protein content than plants with C3 pathway (Young et al.,
492 2016). Also, the reports of C4 or C4-like pathway in marine algae have increased in the last years

https://doi.org/10.5194/bg-2021-50
Preprint. Discussion started: 9 March 2021


493 (Roberts et al., 2007; Doubnerová and Ryslavá, 2011; Xu et al.., 2012, 2013).

494 High activity of keys enzymes of C4 metabolism, such as pyruvate orthophosphate dikinase (PPDK),
495 phosphoenolpyruvate carboxylase (PEPC), and phosphoenolpyruvate carboxykinase (PCK), has
496 been described in macroalgae species. The establishment of a true C4 pathway in marine algae is not
497 clear since the massive changes in gene expression patterns seem to be no complete and it is
498 suggested that many marine algae have high plasticity to use a combination of CCM to overcome Ci
499 limitations (Roberts et al., 2007; Doubnerová and Ryslavá, 2011; Xu et al.., 2012, 2013). A Stepwise
500 model of the path from C3 to C4 photosynthesis is explained in Gowik and Westhoff (2011).

501 An elevated $\delta^{13}C$ signal in macroalgae can also be associated to calcifying species. For instance, in
502 our study, the genus *Amphiroa* and *Jania* both Rhodophyta with articulated-form, averaged -
503 7.86±3.7‰ and -9.37±0.75‰, respectively, which suggest the activity of a CCM using $HCO_3^-$
504 efficiently. Stepien (2015) reported a global mean of -14.83±1.0‰ for calcifying species compared
505 to -20.11±0.31‰ for non-calcifying species. High $\delta^{13}C$ values for calcifying species are related to
506 the excess of $H^+$ released as residuals products of the calcifying process, the acidified boundary
507 layers benefit the $HCO_3^-$ uptake (McConnaughey & Whelan 1997, Courneau et a., 2012). The high
508 δ13C values can also be related to the highly efficient light properties enhanced in the carbonate
509 skeleton, resulting in an optimization of photosynthetic activity (Vasquez-Elizondo et al., 2016,
510 2017). Hofmann and Heesch (2018) reported high $\delta^{13}C$ values in eight rhodoliths species (calcifying
511 species) collected in deep habitats (25-40m) where light availability is low. High $\delta^{13}C$ has been
512 reported for other calcifying species (e.g., *Halimeda, Udotea, Penicillus* with $\delta^{13}C$ usually >10‰)
513 inhabiting seagrass meadows, where the light availability is limited by the *Thalassia testudinum*
514 canopy structure (Berger, 1981; Aharon, 1990; Oehlert et al., 2012; Enríquez et al., 2019). Another
515 case is *Padina* (frondose), a genus with lesser capacity to precipitate $CaCO_3$, but that show relatively

https://doi.org/10.5194/bg-2021-50
Preprint. Discussion started: 9 March 2021


high $\delta^{13}C$ values (-12.49±2.48‰) (Ilus et al., 2017).

According to our fitted regression model to explain the variability of $\delta^{13}C$ by genera can be classified from high (e.g. *Schizymenia* = -19.09‰), moderate (e.g., *Hydroclathrus =7.33‰*; *Amphiroa* = 6.84‰) and low variability (e.g. *Gracilaria* = -0.89; *Spyridia* = -1.46‰). Most species belong into the moderate category, and these range of $\delta^{13}C$ values found is similar to those reported for algae growing up between saturating (less negative values) or sub-saturating light intensity (more negative values) (Hu et al., 2012; Rautemberger et al., 2015; Kübler and Dungeon, 2015). For instance, experimental evidence by Rautemberger et al. (2015) showed *Ulva prolifera* growing under saturated light at different $pCO_2$ levels showed the highest growth rates and activity of internal carbonic anhydrase reached $\delta^{13}C$ signal >-10‰, higher than signal under low light regimen at same $pCO_2$ level. The authors concluded that CCM activity is energy and light dependent. Also, Kübler and Dudgeon (2015) reported that pCO2 and temperature depend on light intensities. Under sub-saturating light intensities, pCO2 has a stronger effect on photosynthetic rates, and the temperature effect increases at saturating light intensities. Light limitation effect on $\delta^{13}C$ signal has been observed in deep subtidal habitats (Mercado et al., 2009; Hepburn et al., 2011; Marconi et al., 2011; Stepien 2015). Nevertheless, our study's shallow water samples' depth was insufficient to find significant differences in δ13C between submareal and intertidal habitats. Even so, according to multivariate linear regression analyses, the emersion level could explain a high percentage of the variability be genus and morpho-functional groups.

Belonging to submareal habitats, we found three non-calcifying species (*Schizymenia pacifica*, *Halymenia* sp., *Gigartina* sp.) of Rhodophyta with negatives values lesser than -30‰, which suggest that are diffusive $CO_2$ users and for hence lack CCM. Their $\delta^{13}C$ signal are consistent with the results of Murru and Sandgreen (2004) whose described *S. pacifica* and two species of *Halymenia* (e.g., *H.*

https://doi.org/10.5194/bg-2021-50
Preprint. Discussion started: 9 March 2021


539 *schizymenioides* and *H. gardner*) as a restricted $CO_2$ user based on measurements of pH drift. Red
540 macroalgae that lack CCM, tend to inhabit in low-light habitats like subtidal or low intertidal and be
541 abundant in cold waters (Kübler et al., 1999, Raven et al., 2002a, Cornwall et al., 2015). According
542 to these authors, approximately 35% of the total red algae tested on a global scale are strictly $CO_2$
543 dependents. Our study evaluated 91 species of 453 red algae species reported in the Gulf of
544 California (Pedroche and Sentíes, 2003), which <3% of red macroalgae specimens could be Ci
545 limited. The low percentage of red macroalgae in the GC lack of CCM, which can be partially
546 explained by the low solubility of $CO_2$ due to relatively high temperatures in subtropical waters
547 (Zeebe & Wolf-Gladrow, 2007). The percentage of macroalgae species representative of Arctic and
548 Antarctic ecosystems is 42-60% (Raven et al., 2002b; Iñiguez et al., 2019), 50% for temperate waters
549 of New Zealand (Hepburn et al., 2011) and until 90% found for a single site of Tazmania Australia
550 (Cornwall et al., 2015). The GC represents close 97%.

551 **4.2. Environment factors and $\delta^{13}C$ values**

552 We expected differences in $\delta^{13}C$ values between eco-regions (e.g., north vs. south, peninsular vs.
553 continental), but non-geographical patterns were observed; neither differences associated with the
554 temperature for the same species o genus was observed. A slightly low $\delta^{13}C$ signal in communities
555 from C2 eco-region was observed, influenced by the Sonora desert.

556 Based on pH, differences in $\delta^{13}C$ were found only for a few genera (e.g., *Amphiroa*, *Colpomenia*,
557 *Ulva*, *Spyridia*), with a trend to increase in the $\delta^{13}C$ values with pH (Maberly et al., 1992, Raven et
558 al. 2002b). Similar results were reported for Cornwall et al. (2017) with the differential response of
559 the $\delta^{13}C$ signals to pH among 19 species, in which only four species were sensitive to pH changes.
560 Our *in-situ* pH measurements do not represent the pH compensation point; the physiology

https://doi.org/10.5194/bg-2021-50
Preprint. Discussion started: 9 March 2021


561 measurement indicates the presence or absence of CCM in photosynthetic organisms. Based on the
562 complete dataset, a weak but significant positive linear regression was observed between $\delta^{13}C$ and
563 pH, similar to the reported by Iñiguez et al. (2009) in three taxa of polar macroalgae. According to
564 Stepien (2015), the result of meta-analyzes between pH values and $\delta^{13}C$ was positive only for
565 Rhodophyta ($R^2$=0.41, p<0.001) and Ochrophyte ($R^2$=0.19, p<0.001), but not for Chlorophyta
566 ($R^2$=0.002, p<0.10). About 86% of the Stepien metadata met the theoretical CCM assignation based
567 on both parameters, exceptions for species with $\delta^{13}C$<-30‰ that has been capable of raising pH>9.

568 Our linear regression analyzes for latitudes showed a weak but significant correlation for the dataset
569 classified by morphofunctional groups and genus, negative in the cases of Rhodophyta and
570 Ochrophyta groups ($R^2$=0.2 and 0.5, p<0.001), and a positive for Chlorophyta. The negative
571 correlation between latitude and $\delta^{13}C$-algal was described by Stepien (2015), concluding that $\delta^{13}C$
572 signal increased by 0.09‰ for each latitude degree from the Equator. Hofmann and Heesch (2018)
573 recently show a strong decrease in latitudinal effect ($R^2$= 0.43 $\delta^{13}C_{total}$ and 0.13, for $\delta^{13}C_{organic\text{-}tissue}$,
574 p=0.001) for rhodolite of the northern hemisphere and macroalgae from coral reefs in Australia. In
575 both cases, the latitude range is higher than we tested (30º to 80º and from 10º to 45º, respectively).
576 These differences on a big scale tend to be associated with a temperature effect (Stepien, 2015) and
577 their effect on CO2 solubility in S.W. (Zeebe & Wolf-Gladrow, 2007). Even so, our multivariate
578 linear regression analyses showed that the environmental factors were significant (p=0.001),
579 explaining up to 50% of the $\delta^{13}C$ variability.

580 **4.3. Morphofunctional groups and $\delta^{13}C$**

581 The variability recorded on morphofunctional groups was high, mostly influenced by the genus. The
582 highest $\delta^{13}C$ values were found in R-larger size articulated y R-smaller-side articulated composed

https://doi.org/10.5194/bg-2021-50
Preprint. Discussion started: 9 March 2021


583 by *Amphiroa* and *Jania* spp, respectively, also O-hollow with spherical composed *Colpomenia* spp.
584 Based on the literature, Stepien (2015) made an analysis about morphofunctional groups and $\delta^{13}C$
585 by following the group proposed by Littler & Littler (1980) and modified by Balata et al., (2012)
586 and they agreed that morphofunctional groups that are composed calcifying species (e.g., crust
587 calcifiers) have highest $\delta^{13}C$ signal. Our regression models showed that morphofunctional groups
588 have a $R^2$ adjusted =0.34, and increase to genus ($R^2$ adjusted =0.41,) and to species ($R^2$ adjusted
589 =0.46). This result is consistent with reported by Lovelock et al., (2020), which found that 66% of
590 $\delta^{13}C$ variability was explained by taxonomy. Although morphofunctional groups could explain less
591 than genus or species, it is a great tool to increase the possibility of analyzes on a big spatial scale,
592 especially when the species distribution could be limited.

593 **5. Conclusions**

594 Our work confirms that taxonomy is the main cause of $\delta^{13}C$ variability among seaweed communities
595 analyzed and explained until 46%. Most species showed a $\delta^{13}C$ belong into a range that indicates a
596 mix of $CO_2$ and $HCO_3^-$ uptake. About 20-34% species depending on cutoff limits for CCM presence
597 showed at least one specimen with $\delta^{13}C$>-10‰, suggesting that potentially could have highly
598 efficient CCM. On the other extreme, some Rhodophyta species relied exclusively on diffusive $CO_2$
599 entry, as inferred from their $\delta^{13}C$ values (i.e. $\delta^{13}C$ lower than -30‰; *Schizymenia pacifica*,
600 *Halymenia* sp., and *Gigartina* sp.). Even so, $\delta^{13}C$ variability associated with species can be classified
601 in high (-19‰), moderate (7‰), low (0.89‰). This variability range is similar to $\delta^{13}C$ values
602 between growing under saturating light (high values) and no saturating (low values). Specimens
603 collected from the subtidal habitat showed more negative $\delta^{13}C$ values (higher discrimination) than
604 the intertidal habitat but without significant difference. The percent of Rhodophyta species (3.26%)
605 that could be Ci limited (without evident CCM activity) is relatively low in comparison that reported

https://doi.org/10.5194/bg-2021-50
Preprint. Discussion started: 9 March 2021


606 for temperate regions (40-90%). The data presented indicate that $HCO_3^-$ uptake by active transport
607 is widespread among GC algae. In this sense, $\delta^{13}C$ provides information about the physiological and
608 environmental status of macroalgae.

609 6. Data Availability Statement

610 Data set are each permanently deposited Soto-Jimenez, MARTIN F; Velázquez-Ochoa, Roberto;
611 Ochoa Izaguirre, Maria Julia. Earth and Space Science Open Archive ESSOAr; Washington, Nov
612 25, 2020. DOI:10.1002/essoar.10504972.1

613 https://search.proquest.com/openview/2060de58b217ca47495469b53ae2f347/1?pq-
614 origsite=gscholar&cbl=4882998

615 **7. Author contribution**

616 Velázquez-Ochoa R. participate in the collection, processing and analysis of the samples as a part
617 of his master's degree thesis. Ochoa-Izaguirre J. also participate in sample collections and
618 identified macroalgae specimens. Soto-Jiménez M.F. coordinated the research, he was the thesis
619 director and prepared the manuscript with contributions from all co-authors.

620 **8. Competing interests**

621 The authors declare that they have no conflict of interest.

622 **9. Acknowledgements**

623 The authors would like to thank H. Bojórquez-Leyva, Y. Montaño-Ley, and A. Cruz-López for
624 their invaluable assistance with field and laboratory work. Thanks to S. Soto Morales for the
625 English revision. UNAM-PAPIIT IN206409 and IN208613 provided financial support and

https://doi.org/10.5194/bg-2021-50
Preprint. Discussion started: 9 March 2021


626 UNAM-PASPA supported to MF Soto-Jimenez for Sabbatical year.

627 **10. References**

628 Abbot, I. A., and Hollenberg, G. Marine algae of California. Standford University Press, California.
629 1976.

630 Aguilar-Rosas, L. E., and R. Aguilar-Rosas, R.: Ficogeografía de las algas pardas (Phaeophyta) de
631 la península de Baja California, in: Biodiversidad Marina y Costera de México (Comisión Nacional
632 Biodiversidad y CIQRO, México), edited by: Salazar-Vallejo, S. I. and González, N. E., 197-206.
633 1993.

634 Aharon, P. Recorders of reef environment histories: stable isotopes in corals, giant clams, and
635 calcareous algae. Coral Reefs., 10(2), 71–90. https://doi.org/10.1007/BF00571826, 1991.

636 Álvarez-Borrego, S.: Gulf of California., in: Ecosystems of the World, 26. *Estuaries and Enclosed*
637 *Seas*, (Elsevier, Amsterdam), Edited by: Ketchum BH., 427–449, 1983.

638 Axelsson, L., Ryberg, H., and Beer, S.: Two modes of bicarbonate utilization in the marine green
639 macroalga *Ulva lactuca*, Plant Cell Environ., 18, 439–445. https://doi.org/10.1111/j.1365-
640 3040.1995.tb00378.x, 1995.

641 Axelsson, L., Larsson, C., and Ryberg, H.: Affinity, capacity and oxygen sensitivity of two different
642 mechanisms for bicarbonate utilization in *Ulva lactuca* L. (Chlorophyta), *Plant Cell Environ.*, 22,
643 969–978. https://doi.org/10.1046/j.1365-3040.1999.00470.x, 1999.

644 Balata, D., Piazzi, L., and Rindi, F.: Testing a new classification of morphological functional groups
645 of marine macroalgae for the detection of responses to stress, Mar. Biol., 158, 2459–2469,
646 https://doi.org/10.1007/s00227-011-1747-y, 2011.

647 Bastidas-Salamanca, M., Gonzalez-Silvera, A., Millán-Núñez, R., Santamaria-del-Angel, E., and
648 Frouin, R.: Bio-optical characteristics of the Northern Gulf of California during June 2008, Int. J.
649 Oceanogra., https://doi.org/10.1155/2014/384618, 2014.

650 Bauwe, H., Hagemann, M., and Fernie, A. R.: Photorespiration: players, partners and origin, Trends
651 Plant Sci., 15(6), 330–336. https://doi.org/10.1016/j.tplants.2010.03.006, 2010.


652 Beardall, J., and Giordano, M.: Ecological implications of microalgal and cyanobacterial $CO_2$
653 concentrating mechanisms, and their regulation, Funct. Plant Biol., 29(3), 335–347.
654 https://doi.org/10.1071/PP01195, 2002.

655 Bold, C. H., and Wynne, J. M.: Introduction to the Algae: Structure and reproduction. Prentice-Hall,
656 Incorporated, 1978.

657 Bowes, G. W.: Carbonic anhydrase in marine algae, Plant Physiol., 44:726–732.
658 https://doi.org/10.1104/pp.44.5.726, 1969.

659 Bray, N. A.: Thermohaline circulation in the Gulf of California, *J. Geophys. Res. Oceans.*, 93(C5),
660 4993–5020. https://doi.org/10.1029/JC093iC05p04993, 1988.

661 Burnham, K. P., and Anderson, D. R.: A practical information-theoretic approach, Model selection
662 and multimodel inference, 2nd ed. Springer, New York, 2. 2002.

663 Carrillo, L., and Palacios-Hernández, E.: Seasonal evolution of the geostrophic circulation in the
664 northern Gulf of California, Estuar. Coast. Shelf Sci., 54(2), 157–173.
665 https://doi.org/10.1006/ecss.2001.0845, 2002.

666 Carvalho, M. C. and Eyre, B. D.: Carbon stable isotope discrimination during respiration in three
667 seaweed species, Mar. Ecol. Prog. Ser., 437:41–49. https://doi.org/10.3354/meps09300, 2011.

668 Cerling, T. E., Wang, Y., and Quade, J.: Expansion of C4 ecosystems as an indicator of global
669 ecological change in the late Miocene, *Nature*, 361 (6410), 344–345,
670 https://doi.org/10.1038/361344a0, 1993.

671 Comeau, S., Carpenter, R. C., and Edmunds, P. J.: Coral reef calcifiers buffer their response to ocean
672 acidification using both bicarbonate and carbonate, *Proc. Bio. Sci.*, 280(1753), 20122374,
673 https://doi.org/10.1098/rspb.2012.2374, 2012.

674 CNA (Comisión Nacional del Agua): Atlas del agua en México, 2012.

675 Cornwall, C. E., Revill, A.T., and Hurd, C. L.: High prevalence of diffusive uptake of $CO_2$ by
676 macroalgae in a temperate subtidal ecosystem, Photosynth. Res., 124, 181–190,
677 https://doi.org/10.1007/s11120-015-0114-0, 2015.

https://doi.org/10.5194/bg-2021-50
Preprint. Discussion started: 9 March 2021


678 Cornwall, C. E., Revill, A. T., Hall-Spencer, J. M., Milazzo, M., Raven, J. A., and Hurd, C. L.:
679 Inorganic carbon physiology underpins macroalgal responses to elevated $CO_2$, *Sci. Rep.*, 7(1), 1–12,
680 https://doi.org/10.1038/srep46297, 2017.

681 Dawson, E. Y.: The marine algae of the Gulf of California, Allan Hancock Pac. Exped., 3(10), [i-
682 v+] 189–453, 1944.

683 Dawson, E. Y.: Marine red algae of Pacific México. Part 2. *Cryptonemiales* (cont.), Allan Hancock
684 Pac. Exped., 17(2), 241–397, 1954.

685 Dawson, E. Y.: How to know the seaweeds, Dubuque, Iowa, USA. W.M.C. Brown. Co. Publishers.
686 pp 197., 1956.

687 Dawson, E. Y.: Marine red algae of Pacific México. Part 7. *Ceramiales*: Ceramiciaceae,
688 Delesseriaceae, Allan Hancock Pac. Exped., 26(1), 1–207, 1962.

689 Dawson, E. Y.: Marine red algae of Pacific México. Part 8. *Ceramiales*: Dasyaceae, Rhodomelaceae.
690 Nova Hedwigia, 6, 437–476, 1963.

691 Doubnerová, V., and Ryšlavá, H.: What can enzymes of C4 photosynthesis do for C3 plants under
692 stress?, *Plant Sci.*, 180(4), 575–583, https://doi.org/10.1016/j.plantsci.2010.12.005, 2011.

693 Draper, N. R., and Smith, H.: Applied regression analysis, edited by: John Wiley & Sons (Vol. 326),
694 1998.

695 Drechsler, Z., and Beer, S.: Utilization of inorganic carbon by *Ulva lactuca*. *Plant Physiol.*, 97,
696 1439–1444, https://doi.org/10.1104/pp.97.4.1439, 1991.

697 Drechsler, Z., Sharkia, R., Cabantchik, Z. I., and Beer, S. Bicarbonate uptake in the marine
698 macroalga *Ulva* sp. is inhibited by classical probes of anion exchange by red blood cells, *Planta*,
699 191(1), 34–40, https://doi.org/10.1007/BF00240893, 1993.

700 Dudgeon, S. R., Davison, I. R., and Vadas, R. L. Freezing tolerance in the intertidal red algae
701 *Chondrus crispus* and *Mastocarpus stellatus:* Relative importance of acclimation and adaptation,
702 Mar Biol., 106(3), 427–436, https://doi.org/10.1007/BF01344323, 1990.

703 Dudley, B. D., Barr, N. G., and Shima, J. S.: Influence of light intensity and nutrient source on $\delta^{13}C$

https://doi.org/10.5194/bg-2021-50
Preprint. Discussion started: 9 March 2021


704 and $\delta^{15}N$ signatures in *Ulva pertusa*, Aquat. Biol., 9(1), 85–93, https://doi.org/10.3354/AB00241,
705 2010.

706 Ehleringer, J. R., Cerling, T. E., and Helliker, B. R.: C4 photosynthesis, atmospheric $CO_2$, and
707 climate, Oecologia, 112(3), 285–299. https://doi.org/10.1007/s004420050311, 1997.

708 Ehleringer, J. R., Sage, R. F., Flanagan, L. B., and Pearcy, R. W.: Climate change and the evolution
709 of C4 photosynthesis, Trends Ecol. Evol., 6(3), 95–99, https://doi.org/10.1073/pnas.1718988115,
710 1991.

711 Enríquez, S., Agustí, S. and Duarte, C.: Light absorption by marine macrophytes, Oecologia,
712 98:121–129, https://doi.org/10.1007/BF00341462, 1994.

713 Enriquez, S., and Sand-Jensen, K.: Variation in light absorption properties of *Mentha aquatica* L. as
714 a function of leaf form: implications for plant growth, *Int. J. Plant Sci.*, 164(1), 125–136,
715 https://doi.org/10.1086/344759, 2003.

716 Enríquez, S., and Rodríguez-Román, A.: Effect of water flow on the photosynthesis of three marine
717 macrophytes from a fringing-reef lagoon, *Mar. Ecol. Prog. Ser.*, 323, 119–132.
718 https://doi.org/10.3354/meps323119, 2006.

719 Enríquez, S., Olivé, I., Cayabyab, N., and Hedley, J. D.: Structural complexity governs seagrass
720 acclimatization to depth with relevant consequences for meadow production, macrophyte diversity
721 and habitat carbon storage capacity, *Sci. Rep*, 9(1), 1–14. https://doi.org/10.1038/s41598-019-51248-
722 z, 2019.

723 Espinoza-Avalos, J.: Macroalgas marinas del Golfo de California, Biodiversidad marina y costera
724 de México (CONABIO- CIQRO, México), edited by: Salazar-Vallejo, S.I., González, N. E., 328–
725 357, 1993.

726 Espinosa-Carreón, T. L., and Valdez-Holguín, E.: Variabilidad interanual de clorofila en el Golfo de
727 California. Ecol. Apl., 6(1-2), 83–92, 2007.

728 Espinosa-Carreón, T. L., and Escobedo-Urías, D.: South region of the Gulf of California large marine
729 ecosystem upwelling, fluxes of $CO_2$ and nutrients, Environ Dev., 22, 42–51.
730 https://doi.org/10.1016/j.envdev.2017.03.005, 2017.

https://doi.org/10.5194/bg-2021-50
Preprint. Discussion started: 9 March 2021


731 Fernández, P. A., Hurd, C. L., and Roleda, M. Y.: Bicarbonate uptake via an anion exchange protein
732 is the main mechanism of inorganic carbon acquisition by the giant kelp *Macrocystis pyrifera*
733 (Laminariales, Phaeophyceae) under variable pH, J. Phycol., 50(6), 998–1008.
734 https://doi.org/10.1111/jpy.12247, 2014.

735 Fernández, P. A., Roleda, M. Y., and Hurd, C. L.: Effects of ocean acidification on the
736 photosynthetic performance, carbonic anhydrase activity and growth of the giant kelp *Macrocystis*
737 *pyrifera*. Photosynth. Res., 124(3), 293–304. https://doi.org/10.1007/s11120-015-0138-5, 2015.

738 Gateau, H., Solymosi, K., Marchand, J., and Schoefs, B.: Carotenoids of microalgae used in food
739 industry and medicine. Mini-Rev. Med. Chem., 17(13), 1140–1172,
740 https://doi.org/10.2174/1389557516666160808123841, 2017.

741 Gilbert, J. Y., and Allen, W. E.: The phytoplankton of the Gulf of California obtained by the ‘‘E.W.
742 Scripps’’ in 1939 and 1940, J. Mar. Res., 5, 89–110, https://doi.org/10.1016/0022-0981(67)90008-
743 1, 1943.

744 Giordano, M., Beardall, J., and Raven, J. A.: $CO_2$ concentrating mechanisms in algae: mechanisms,
745 environmental modulation and evolution, Annu. Rev. Plant Biol., 66:99–131,
746 https://doi.org/10.1146/annurev.arplant.56.032604.144052, 2005.

747 Gowik, U., and Westhoff, P.: The path from C3 to C4 photosynthesis, Plant Physiol., 155(1), 56–63,
748 https://doi.org/10.1104/pp.110.165308, 2012.

749 Grime, J. P.: Evidence for the existence of three primary strategies in plants and its relevance to
750 ecological and evolutionary theory, Am Nat, 111(982), 1169–1194, 1977.

751 Hepburn, C. D., Pritchard, D. W., Cornwall, C. E., McLeod, R. J., Beardall, J., Raven, J. A., and
752 Hurd, C. L.: Diversity of carbon use strategies in a kelp forest community: implications for a high
753 $CO_2$ ocean, Glob. Change Biol., 17, 2488–2497. https://doi.org/10.1111/j.1365-2486.2011.02411.x.,
754 2011.

755 Hofmann, L., and Heesch, S.: Latitudinal trends in stable isotope signatures and carbon-
756 concentrating mechanisms of northeast Atlantic rhodoliths, Biogeosciences, 15, 6139–6149,
757 https://doi.org/10.5194/bg-15-6139-2018, 2018.

https://doi.org/10.5194/bg-2021-50
Preprint. Discussion started: 9 March 2021


758 Hopkinson, B. M., Dupont, C. L., Allen, A. E., and Morel, F. M. M.: Efficiency of the $CO_2$-
759 concentrating mechanism of diatoms, Proc. Natl. Acad. Sci. U.S.A., 108, 3830–3837.
760 https://doi.org/10.1073/pnas.1018062108, 2011.

761 Hopkinson, B. M., Young, J. N., Tansik, A. L., and Binder, B. J.: The minimal $CO_2$ concentrating
762 mechanism of *Prochlorococcus* MED4 is effective and efficient, *Plant Physiol.*, 166, 2205–2217,
763 https://doi.org/10.1104/pp.114.247049, 2014.

764 Hu, X., Burdige, D. J., and Zimmerman, R. C.: $\delta^{13}C$ is a signature of light availability and
765 photosynthesis in seagrass, Limnol. Oceanogr., 57(2), 441–448,
766 https://doi.org/10.4319/lo.2012.57.2.0441, 2012.

767 Hurd, C.L.: Water motion, marine macroalgal physiology, and production, J. Phycol., 36, 453–472,
768 https://doi.org/10.1046/j.1529-8817.2000.99139.x, 2000.

769 Iluz, D., Fermani, S., Ramot, M., Reggi, M., Caroselli, E., Prada, F., Dubinsky, Z., Goffredo, S. and
770 Falin, G.:Calcifying response and recovery potential of the brown alga *Padina pavonica* under ocean
771 acidification, ACS Earth Space Chem., 1(6), 316–323,
772 https://doi.org/10.1021/acsearthspacechem.7b00051, 2017.

773 Iñiguez, C., Galmés, J., and Gordillo, F. J.: Rubisco carboxylation kinetics and inorganic carbon
774 utilization in polar versus cold-temperate seaweeds, J. Exp. Bot., 70(4), 1283–1297.
775 https://doi.org/10.1093/jxb/ery443, 2019.

776 Jensen, E. L., Maberly, S. C., and Gontero, B.: Insights on the functions and ecophysiological
777 relevance of the diverse carbonic anhydrases in microalgae, Int. J. Mol. Sci., 21(8), 2922,
778 https://doi.org/10.3390/ijms21082922, 2020.

779 Kim, M. S., Lee, S. M., Kim, H. J., Lee, S. Y., Yoon, S. H., and Shin, K. H.: Carbon stable isotope
780 ratios of new leaves of *Zostera marina* in the mid-latitude region: implications of seasonal variation
781 in productivity, J. Exp. Mar Biol. Ecol., 461, 286–296. https://doi.org/10.1016/j.jembe.2014.08.015,
782 2014.

783 Kirk, J. T. O.: Light and Photosynthesis in Aquatic Ecosystems, 3rd ed. Cambridge University Press,
784 Cambridge, 2011.

https://doi.org/10.5194/bg-2021-50
Preprint. Discussion started: 9 March 2021


785 Klenell, M., Snoeijs, P., and Pedersen, M. Active carbon uptake in *Laminaria digitata* and *L.*
786 *saccharina* (Phaeophyta) is driven by a proton pump in the plasma membrane. *Hydrobiologia*, 514,
787 41–53. https://doi.org/10.1023/B:hydr.0000018205.80186.3e, 2004.

788 Kremer, B. P.: Metabolic implications of non-photosynthetic carbon fixation in brown macroalgae,
789 *Phycologia*, 20(3), 242–250. https://doi.org/10.2216/i0031-8884-20-3-242.1, 1981.

790 Kübler, J. E., and Davison, I. R.: High-temperature tolerance of photosynthesis in the red alga
791 *Chondrus crispus*, Mar. Biol., 117(2), 327–335. https://doi.org/10.1007/BF00345678, 1993.

792 Kübler, J., Johnston, E., Andrew, M., and Raven, J. A.: The effects of reduced and elevated $CO_2$ and
793 $O_2$ on the seaweed *Lomentaria articulate*, Plat Cell Environ., 22, 1303–1310,
794 https://doi.org/10.1046/j.1365-3040.1999.00492.x, 1999.

795 Kübler, J. E., and Dudgeon, S. R.: Predicting effects of ocean acidification and warming on algae
796 lacking carbon concentrating mechanisms, *PLoS One*, 10 (7),
797 https://doi.org/10.1371/journal.pone.0132806, 2015.

798 Küppers, U., and Kremer, B. P.: Longitudinal profiles of carbon dioxide fixation capacities in marine
799 macroalgae, Plant Physiol., 62(1), 49–53, https://doi.org/10.1104/pp.62.1.49, 1978.

800 Kustka, A. B., Milligan, A. J., Zheng, H., New, A. M., Gates, C., Bidle, K. D., and Reinfelder, J. R.:
801 Low $CO_2$ results in a rearrangement of carbon metabolism to support C4 photosynthetic carbon
802 assimilation in *Thalassiosira pseudonana*, New Phytol. 204(3), 507–520.
803 https://doi.org/10.1111/nph.12926, 2014.

804 Lapointe, B. E., and Duke, C. S.: Biochemical strategies for growth of *Gracilaria tikvahiae*
805 (Rhodophyta) in relation to light intensity and nitrogen availability, J. Phycol., 20(4), 488–495.
806 https://doi.org/10.1111/j.0022-3646.1984.00488.x, 1984.

807 Littler, M. M., and Littler, D. S.: The evolution of thallus form and survival strategies in
808 benthic marine macroalgae: field and laboratory tests of a functional form model, Am Nat.,
809 116, 25–44, 1980.

https://doi.org/10.5194/bg-2021-50
Preprint. Discussion started: 9 March 2021


Littler, M. M., and Arnold, K. E.: Primary productivity of marine macroalgal functional-form groups from south-western North America, J. Phycol., 18, 307–311, https://doi.org/10.1111/j.1529-8817.1982.tb03188.x, 1982.

Littler, M.M., and Littler, D.S.: Relationships between macroalgal functional form groups and substrata stability in subtropical rocky intertidal system, J. Exp. Mar. Biol. Ecol., 74, 13–34, https://doi.org/10.1016/0022-0981(84)90035-2, 1984.

Lovelock, C. E., Reef, R., Raven, J. A., and Pandolfi, J. M., Regional variation in $\delta^{13}C$ of coral reef macroalgae. Limnol. Oceanogr, https://doi.org/10.1002/lno.11453, 2020.

Lluch-Cota, S. E., Aragon-Noriega, E. A., Arreguin-Sanchez, F., Aurioles-Gamboa, D., Bautista-Romero, J. J., Brusca, R. C., Cervantes-Duarte, R., Cortes-Altamirano, R., Del-MonteLuna, P., Esquivel-Herrera, A., Fernandez, G., Hendrickx, M. E., Hernandez-Vazquez, S., Herrera-Cervantes, H., Kahru, M., Lavin, M., Lluch-Belda, D., Lluch-Cota, D. B., Lopez-Martinez, J., Marinone, S. G., Nevarez-Martinez, M. O., Ortega-Garcia, S., Palacios-Castro, E., Pares-Sierra, A., Ponce-Diaz, G., RamirezRodriguez, M., Salinas-Zavala, C. A., Schwartzlose, R. A., and Sierra-Beltran, A. P.: The Gulf of California: Review of ecosystem status and sustainability challenges, Prog. Oceanogr., 73, 1–26, 2007.

Maberly, S. C., Raven, J. A. and Johnston, A. M.: Discrimination between $^{12}C$ and $^{13}C$ by marine plants, *Oecologia,* 91,481–492, https://doi.org/10.1007/BF00650320, 1992.

Madsen, T. V., and Maberly, S. C.: High internal resistance to $CO_2$ uptake by submerged macrophytes that use $HCO_3^-$: measurements in air, nitrogen and helium. Photosynth. Res., 77(2-3), 183–190. https://doi.org/10.1023/A:1025813515956, 2003.

Marinone, S. G., and Lavín, M. F.: Residual flow and mixing in the large islands' region of the central Gulf of California: Nonlinear processes in geophysical fluid dynamics, Springer, Dordrechm, http://doi-org-443.webvpn.fjmu.edu.cn/10.1007/978-94-010-0074-1_13, 2003.

Marinone, S. G.: A note on "Why does the Ballenas Channel have the coldest SST in the Gulf of California?". *Geophysical research letters*, 34(2). https://doi.org/10.1029/2006GL028589, 2007.


839 Marconi, M., Giordano, M., and Raven, J. A.: Impact of taxonomy, geography and depth on the $\delta^{13}C$
840 and $\delta^{15}N$ variation in a large collection of macroalgae, J. Phycol., 47, 1023–1035,
841 https://doi.org/10.1111/j.1529-8817.2011.01045.x, 2011.

842 Marshall, J. D., Brooks, J. R., and Lajtha, K.: Sources of variation in the stable isotopic composition
843 of plants: Stable isotopes in ecology and environmental science, 2, 22–60.
844 https://doi.org/10.1002/9780470691854.ch2, 2007.

845 Martínez-Díaz-de-León, A.: Upper-ocean circulation patterns in the Northern Gulf of California,
846 expressed in Ers-2 synthetic aperture radar imagery, Cienc. Mar., 27(2), 209–221.
847 https://doi.org/10.7773/cm.v27i2.465, 2001.

848 Martínez-Díaz-de-León, A., Pacheco-Ruíz, I., Delgadillo-Hinojosa, F., Zertuche-González, J. A.,
849 Chee-Barragán, A., Blanco-Betancourt, R., Guzmán-Calderón, J. M., and Gálvez-Telles, A.: Spatial
850 and temporal variability of the sea surface temperature in the Ballenas-Salsipuedes Channel (central
851 Gulf of California), J. Geophys. Res. Oceans, 111(C2), https://doi.org/10.1029/2005JC002940,
852 2006.

853 Masojidek, J., Kopecká, J., Koblížek, M., and Torzillo, G.: The xanthophyll cycle in green algae
854 (Chlorophyta): its role in the photosynthetic apparatus. Plant Biol., 6(3), 342–349,
855 https://doi.org/10.1055/s-2004-820884, 2004.

856 McConnaughey, T. A., Burdett, J., Whelan, J. F., and Paull, C. K.: Carbon isotopes in biological
857 carbonates: respiration and photosynthesis, Geochim. Cosmochim Ac., 61(3), 611–622,
858 https://doi.org/10.1016/S0016-7037(96)00361-4, 1997.

859 Mercado, J. M., De los Santos, C. B., Pérez-Lloréns, J. L., and Vergara, J. J.: Carbon isotopic
860 fractionation in macroalgae from Cadiz Bay (Southern Spain): comparison with other bio-
861 geographic regions, Estuar, Coast. Shelf Sci., 85, 449–458,
862 https://doi.org/10.1016/j.ecss.2009.09.005, 2009.

863 Murru, M. and Sandgren, C. D.: Habitat matters for inorganic carbon acquisition in 38 species of red
864 macroalgae (Rhodophyta) from Puget Sound, Washington, USA. J. Phycol., 40, 837–845.
865 https://doi.org/10.1111/j.1529-8817.2004.03182.x, 2004.

https://doi.org/10.5194/bg-2021-50
Preprint. Discussion started: 9 March 2021


866 Nielsen, S. L., and Jensen, K. S.: Allometric settling of maximal photosynthetic growth rate to
867 surface/volume ratio, *Limnol. Oceanogra.*, 35(1), 177–180,
868 https://doi.org/10.4319/lo.1990.35.1.0177, 1990.

869 Norris, J. N.: Marine algae of the northern Gulf of California: Chlorophyta and Phaoephyceae,
870 Smithsonian contr. Bot., no. 94, https://doi.org/10.5479/si.19382812.96, 2010.

871 Oehlert, A. M., Lamb-Wozniak, K. A., Devlin, Q. B., Mackenzie, G. J., Reijmer, J. J., and
872 Swart, P. K.: The stable carbon isotopic composition of organic material in platform derived
873 sediments: implications for reconstructing the global carbon cycle, Sedimentology, 59(1),
874 319–335. https://doi.org/10.1111/j.1365-3091.2011.01273.x, 2012.
875
876 Ochoa-Izaguirre, M. J., Aguilar-Rosas, R., and Aguilar-Rosas, L. E.: Catálogo de Macroalgas de las
877 lagunas costeras de Sinaloa. Serie Lagunas Costeras, Edited by Páez-Osuna, F., UNAM, ICMyL,
878 México, pp 117, 2007.

879 Ochoa-Izaguirre, M. J., and Soto-Jiménez, M. F.: Variability in nitrogen stable isotope ratios
880 of macroalgae: consequences for the identification of nitrogen sources, J. Phycol., 51, 46–
881 65. https://doi.org/10.1111/jpy.12250, 2015.
882
883 O'Leary, M. H.: Carbon isotopes in photosynthesis, Bioscience, *38*(5), 328–336.
884 https://doi.org/10.2307/1310735, 1988.
885
886 O'Leary, M. H.: Biochemical basis of carbon isotope fractionation: Stable isotopes and plant
887 carbon-water relations, edited by Academic Press, https://doi.org/10.1016/B978-0-08-
888 091801-3.50009-X, 1993.
889 Páez-Osuna, F., Álvarez-Borrego, S., Ruiz-Fernández, A. C., García-Hernández, J., Jara-
890 Marini, E., Bergés-Tiznado, M. E., Piñón-Gimate, A., Alonso-Rodríguez, R., Soto-Jiménez,
891 M. F., Frías-Espericueta, M. G., Ruelas-Inzunza, J. R., Green-Ruíz, C. R., Osuna-Martínez,
892 C. C., and Sánchez-Cabeza, J. A.: Environmental status of the Gulf of California: a pollution
893 review, *Earth-Sci. Rev.*, 166, 181–205. https://doi.org/10.1016/j.earscirev.2016.09.015,
894 2017.
895

https://doi.org/10.5194/bg-2021-50
Preprint. Discussion started: 9 March 2021


896 Pärtel, M., Laanisto, L., and Zobel, M.: Contrasting plant productivity–diversity relationships
897 across latitude: the role of evolutionary history, Ecology, 88(5), 1091–1097,
898 https://doi.org/10.1890/06-0997, 2007.
899
900 Pärtel, M., and Zobel, M.: Dispersal limitation may result in the unimodal productivity-
901 diversity relationship: a new explanation for a general pattern, J. Ecol., 95(1), 90–94,
902 https://doi.org/10.1111/j.1365-2745.2006.01185.x, 2007.
903
904 Pedroche, F. F., and Sentíes, A.: Ficología marina mexicana: Diversidad y Problemática
905 actual, *Hidrobiológica*, 13(1), 23–32, 2003.
906
907 Rautenberger, R., Fernandez, P. A., Strittmatter, M., Heesch, S., Cornwall, C. E., Hurd, C. L., and
908 Roleda, M. Y.: Saturating light and not increased carbon dioxide under ocean acidification drive
909 photosynthesis and growth in *Ulva rigida* (Chlorophyta), Ecol. Evol., 5(4), 874–888,
910 https://doi.org/10.1002/ece3.1382, 2015.

911 Raven, J. A., Johnston, A. M., Kübler, J. E., Korb, R. E., McInroy, S. G., Handley, L. L., Scrimgeour,
912 C. M., Walker, D. I., Beardall, J., Clayton, M. N., Vanderklift, M., Fredriksen, S., Dunton, K. H.:
913 Seaweeds in cold seas: evolution and carbon acquisition. Ann. Bot., 90, 525–536.
914 https://doi.org/10.1093/aob/mcf171, 2002a.

915 Raven, J. A., Johnshton, A. M., Kübler, J. E., Korb, R. E., Mclnroy, S. G., Handley, L. L.,
916 Scrimgeour, C. M., Walker, D. I., Beardall, J., Vanderklift, M., Fredriksen, S., Dunton, K. H.:
917 Mechanistic interpretation of carbon isotope discrimination by marine macroalgae and seagrasses,
918 Funct. Plant Biol., 29:355–378. https://doi.org/10.1071/PP01201, 2002b.

919 Raven, J. A., Ball, L. A., Beardall, J., Giordano, M., and Maberly, S. C.: Algae lacking carbon-
920 concentrating mechanisms, Can. J. Bot., 83(7), 879–890, https://doi.org/10.1139/b05-074, 2005.

921 Raven, J. A., and Hurd, C.: Ecophysiology of photosynthesis in macroalgae, Photosynth. Res., 113,
922 105–125, https://doi.org/10.1007/s11120-012-9768-z, 2012.

923 Raven, J. A., and Beardall, J.: The ins and outs of $CO_2$, J. Exp. Bot., *67*(1), 1–13,
924 https://doi.org/10.1093/jxb/erv451, 2016.

https://doi.org/10.5194/bg-2021-50
Preprint. Discussion started: 9 March 2021


925

926 Reiskind, J. B., Seamon, P. T., and Bowes, G.: Alternative methods of photosynthetic carbon
927 assimilation in marine macroalgae, Plant Physiol., 87, 686–692, https://doi.org/10.1104/pp.87.3.686,
928 1988.

929 Reiskind, J. B., and Bowes, G.: The role of phosphoenolpyruvate carboxykinase in a marine
930 macroalga with C4-like photosynthetic characteristics, PNAS USA, 88, 2883–2887,
931 https://doi.org/10.1073/pnas.88.7.2883, 1991.

932 Roberts, K., Granum, E., Leegood, R. C., and Raven, J. A.: C3 and C4 pathways of photosynthetic
933 carbon assimilation in marine diatoms are under genetic, not environmental control, Plant Physiol.,
934 145(1), 230–235, https://doi.org/10.1104/pp.107.102616, 2007.

935 Roden, G. I., and Groves, G. W.: Recent oceanographic investigations in the Gulf of California, J.
936 Mar. Res., 18(1), 10–35, 1959.

937 Roden, G. I., and Emilsson, L.: Physical oceanography of the Gulf of California. Simposium Golfo
938 de California, Universidad Nacional Autónoma de México, Mazatlán, Sinaloa, México, 1979.

939 Rusnak, G. A., Fisher, R. L., and Shepard, F. P.: Bathymetry and faults of Gulf of California. In: van
940 Andel, Tj. H. and G.G. Shor, Jr. (editors). Marine Geology of the Gulf of California: A symposium,
941 *AAPG Memoir*, 3, 59–75. https://doi.org/10.1306/M3359C3, 1964.

942 Santamaría-del-Angel, E., Alvarez-Borrego, S., and Müller-Karger, F. E.: Gulf of California
943 biogeographic regions based on coastal zone color scanner imagery, J. Geophys. Res., 99,
944 7411–7421, https://doi.org/10.1029/93JC02154, 1994.

945

946 Sanford, L. P., and Crawford, S. M.: Mass transfer versus kinetic control of uptake across solid-
947 water boundaries, Limnol. Oceanogr., 45, 1180−1186, https://doi.org/10.4319/lo.2000.45.5.1180,
948 2000.

949 Sand-Jensen, K., and Gordon, D.: Differential ability of marine and freshwater macrophytes to utilize
950 $HCO_3^-$ and $CO_2$, Mar. Biol., 80, 247–253, https://doi.org/10.1111/j.1469-8137.1981.tb03198.x,
951 1984.

https://doi.org/10.5194/bg-2021-50
Preprint. Discussion started: 9 March 2021


952 Setchell, W., and Gardner, N.: The marine algae of the Pacific Coast of North America. Part II
953 Chlorophyceae, Univ. Calif. Publ. Bot., 8, 139–374, https://doi.org/10.5962/bhl.title.5719, 1920.
954
955 Setchell, W., and Gardner, N.: The marine algae: Expedition of the California Academy of Sciences
956 to the Gulf of California in 1921, Proc. Calif. Acad. Sci., *4th series*, 12(29), 695–949, 1924.

957 Sharkey, T. D., and Berry, J. A.: Carbon isotope fractionation of algae as influenced by an inducible
958 $CO_2$ concentrating mechanism. Inorganic carbon uptake by aquatic photosynthetic organisms, 1985.

959 Stepien, C. C.: Impacts of geography, taxonomy and functional group on inorganic carbon use
960 patterns in marine macrophytes, J. Ecol., 103(6), 1372–1383, https://doi.org/10.1111/1365-
961 2745.12451, 2015.

962 Stepien, C. C., Pfister, C. A., and Wootton, J. T.: Functional traits for carbon access in macrophytes.
963 PloS one, 11(7), e0159062, https://doi.org/10.1371/journal.pone.0159062, 2016.

964 Valiela, I., Liu, D., Lloret, J., Chenoweth, K., and Hanacek, D.: Stable isotopic evidence of
965 nitrogen sources and C4 metabolism driving the world's largest macroalgal green tides in the
966 Yellow Sea, Sci. Rep., 8(1), 1–12. https://doi.org/10.1038/s41598-018-35309-3, 2018.
967
968 Vásquez-Elizondo, R. M., Legaria-Moreno, Pérez-Castro, M.A., Krämer, W. E., Scheufen, T.,
969 Iglesias-Prieto, R., and Enríquez, S.: Absorptance determinations on multicellular tissues,
970 Photosynth, Res., 132, 311–324, https://doi.org/10.1007/s11120-017-0395-6, 2017.

971 Vásquez-Elizondo, R. M., and Enríquez, S.: Light absorption in coralline algae (Rhodophyta): a
972 morphological and functional approach to understanding species distribution in a coral reef lagoon,
973 Front. Mar. Sci., 4, 297, https://doi.org/10.3389/fmars.2017.00297, 2017.

974 Velasco-Fuentes, O. V., and Marinone, S. G.: A numerical study of the Lagrangian circulation in the
975 Gulf of California, J. Mar. Syst., 22(1), 1–12. https://doi.org/10.1016/S0924-7963(98)00097-9,
976 1999.

977 Young, E. B., and Beardall, J.: Modulation of photosynthesis and inorganic carbon acquisition in a
978 marine microalga by nitrogen, iron, and light availability, Can. J. Bot., 83(7), 917–928,
979 https://doi.org/10.1139/b05-081, 2005.

https://doi.org/10.5194/bg-2021-50
Preprint. Discussion started: 9 March 2021


980 Young, J. N., Heureux, A. M., Sharwood, R. E., Rickaby, R. E., Morel, F. M., and Whitney, S. M.:
981 Large variation in the Rubisco kinetics of diatoms reveals diversity among their carbon-
982 concentrating mechanisms, J. Exp. Bot., 67(11), 3445–3456, https://doi.org/10.1093/jxb/erw163,
983 2016.

984 Xu, J., Fan, X., Zhang, X., Xu, D., Mou, S., Cao, S., Zheng, Z., Miao, J., Ye, N.: Evidence of
985 coexistence of C3 and C4 photosynthetic pathways in a green-tide-forming alga, *Ulva prolifera*,
986 *PloS one*, 7(5), e37438, https://doi.org/10.1371/journal.pone.0037438, 2012.

987 Xu, J., Zhang, X., Ye, N., Zheng, Z., Mou, S., Dong, M., Xu, D. and Miao, J.: Activities of principal
988 photosynthetic enzymes in green macroalga *Ulva linza*: functional implication of C4 pathway in $CO_2$
989 assimilation, Sci. China Life Sci., 56(6), 571–580, https://doi.org/10.1007/s11427-013-4489-x,
990 2013.

991 Wefer, G., and Berger, W. H.: Stable isotope composition of benthic calcareous algae from Bermuda,
992 J. Sediment. Res., 51(2), 459–465, https://doi.org/10.1306/212F7CAC-2B24-11D7-
993 8648000102C1865D, 1981.

994 Wilkinson T. E., Wiken, J., Bezaury-Creel, T., Hourigan, T., Agardy, H., Herrmann, L., Janishevski,
995 C. Madden, L. Morgan and M. Padilla.: Marine Ecoregions of North America. CEC, Montreal,
996 Canada, 2009.

997 Zabaleta, E., Martin, M. V., and Braun, H. P.: A basal carbon concentrating mechanism in plants?,
998 Plant Sci., 187, 97–104, https://doi.org/10.1016/j.plantsci.2012.02.001, 2012.

999 Zeebe, R. E., and Wolf-Gladrow, D.: $CO_2$ in seawater: equilibrium, kinetics, isotopes (No. 65) Gulf
1000 Professional Publishing, 2001.

1001 Zeitzschel, B.: Primary productivity in the Gulf of California, Mar. Biol., 3(3), 201–207,
1002 https://doi.org/10.1007/BF00360952, 1969.

1003 Zhou, L., Gao, S., Huan, L., Wu, S., Wang, G., and Gu, W.: Enzyme activities suggest that the NAD-
1004 ME C4 type CCM exist in *Ulva* sp., Algal Res., 47, 101809,
1005 https://doi.org/10.1016/j.algal.2020.101809, 2020.

1006 Zou, D., Xia, J., and Yang, Y.: Photosynthetic use of exogenous inorganic carbon in the agarophyte

https://doi.org/10.5194/bg-2021-50
Preprint. Discussion started: 9 March 2021


1007 *Gracilaria lemaneiformis* (Rhodophyta), Aquaculture, 237, 421-431,
1008 https://doi.org/10.1016/j.aquaculture.2004.04.020, 2004.

1009

1010 **Figure captions**

1011 Fig. 1. Sites collection along the continental (C1-C3) and peninsula (P1-P3) Gulf of California
1012 coastlines (A), range of environmental factors supporting or limiting the life processes for the
1013 macroalgal communities within a habitat (B), and inserted Table with the features and
1014 environmental conditions in the diverse habitats in the GC ecoregion that delimits the macroalgal
1015 community's zonation.

1016 Fig. 2. Variability $\delta^{13}C$ values for specimens of different macroalgae genera collected along GC
1017 coastlines classified by taxon, Chlorophyta and Ochrophyta (a) and Rhodophyta (b). Different
1018 letters indicate significant differences ($P<0.05$): a>b>c>d>e.

1019 Fig. 3. Variability $\delta^{13}C$ values for the most representative genus collected along continental (C1 to
1020 C3) and peninsula (P1 to P3) coastline of the Gulf of California.

1021 Fig. 4. Variability of $\delta^{13}C$ values in macroalgae specimens for the most representative genera in
1022 function of habitat features (emersion level).

https://doi.org/10.5194/bg-2021-50
Preprint. Discussion started: 9 March 2021


1023 Fig. 5. Variability of $\delta^{13}C$ values in macroalgae specimens for the most representative genus in
1024 function of temperature (a) and pH (b) ranges in samples collected along continental (C1-C3) and
1025 peninsula (P1-P3) Gulf of California coastline.

1026 Fig. 6. Trends in the $\delta^{13}C$-macroalgal from GC along latitude gradients for genus classified by
1027 phyla Chlorophyta (a), Ochrophyta (b), and Rhodophyta (c). Solid lines indicate the significant
1028 relationships with $P<0.05$.

1029 Fig. 7. Trends in the $\delta^{13}C$-macroalgal in specimens collected along continental (C1-C3) and
1030 peninsula (P1-P3) Gulf of California coastline in function of pH in seawater.

https://doi.org/10.5194/bg-2021-50
Preprint. Discussion started: 9 March 2021




1031

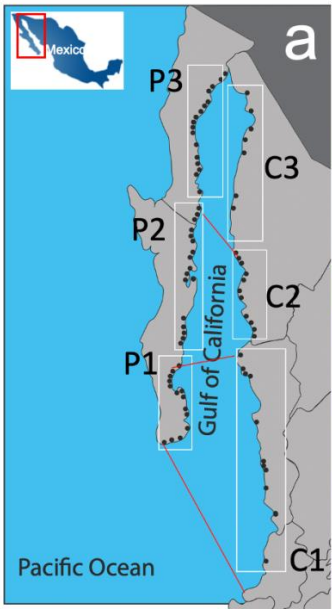


Habitats features and environmental conditions in sampling sites

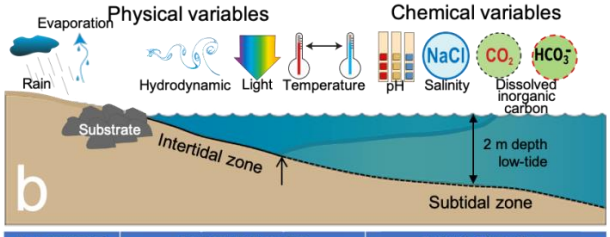


| Environmental factors | Continental GC coastline | | | Peninsula GC coastline | | |
|---|---|---|---|---|---|---|
| | C1 | C2 | C3 | P1 | P2 | P3 |
| Substrate at shores | Rocky and sandy-rocky | Only sandy-rocky shore | Rocky and sandy-rocky | Rocky and sandy-rocky | Rocky and sandy-rocky | Rocky and sandy-rocky |
| Hydrodynamic (water movement) | Slow to fast | Slow to fast | Slow to fast | Slow to fast | Slow to fast | Slow to fast |
| Protection level sites | Exposed and protected | Exposed and protected | Exposed and protected | Exposed and protected | Exposed and protected | Exposed and protected |
| Immersion level | Intertidal and subtidal | Intertidal and subtidal | Intertidal and subtidal | Intertidal and subtidal | Intertidal and subtidal | Intertidal and subtidal |
| pH ranges | Acid, typical and alkaline | Acid, typical and alkaline | Acid, typical and alkaline | Acid, typical and alkaline | Typical and alkaline | Acid, typical and alkaline |
| Temperature ranges | Typical and warmer | Colder, typical and warmer | Colder, typical and warmer | Colder, typical and warmer | Colder, typical and warmer | Colder, typical and warmer |
| Salinity ranges | Marine | Hypersaline, marine, estuarine | Marine | Marine | Marine | Marine |

1032

1033 Fig. 1

https://doi.org/10.5194/bg-2021-50
Preprint. Discussion started: 9 March 2021




1034

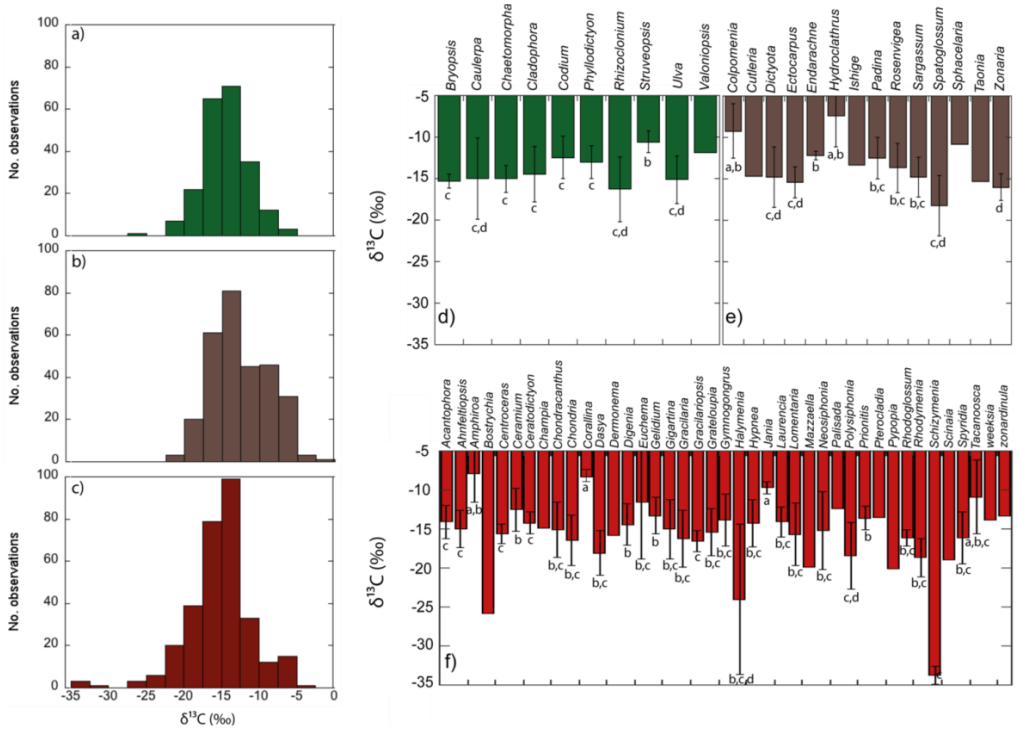


1035

1036 Fig 2

https://doi.org/10.5194/bg-2021-50
Preprint. Discussion started: 9 March 2021




1037

1038

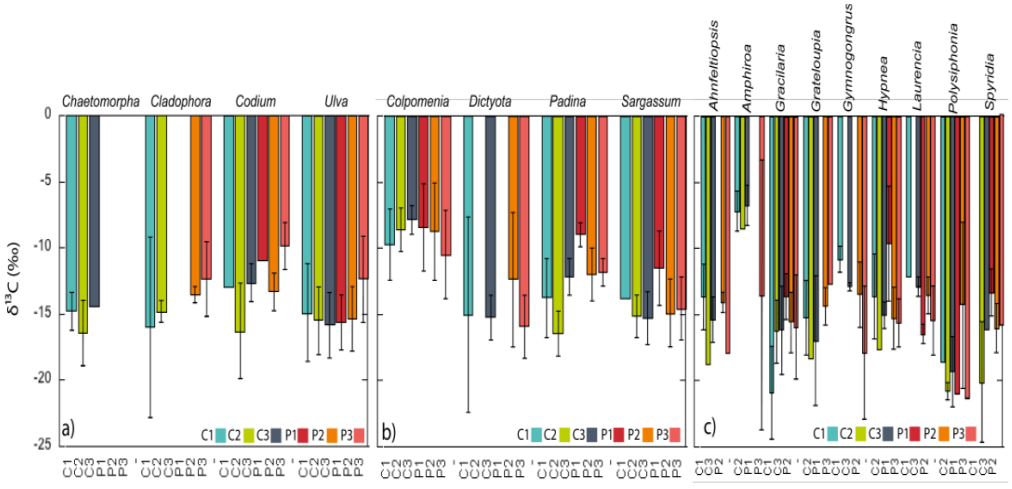


1039
1040 **Fig 3**

https://doi.org/10.5194/bg-2021-50
Preprint. Discussion started: 9 March 2021




1041

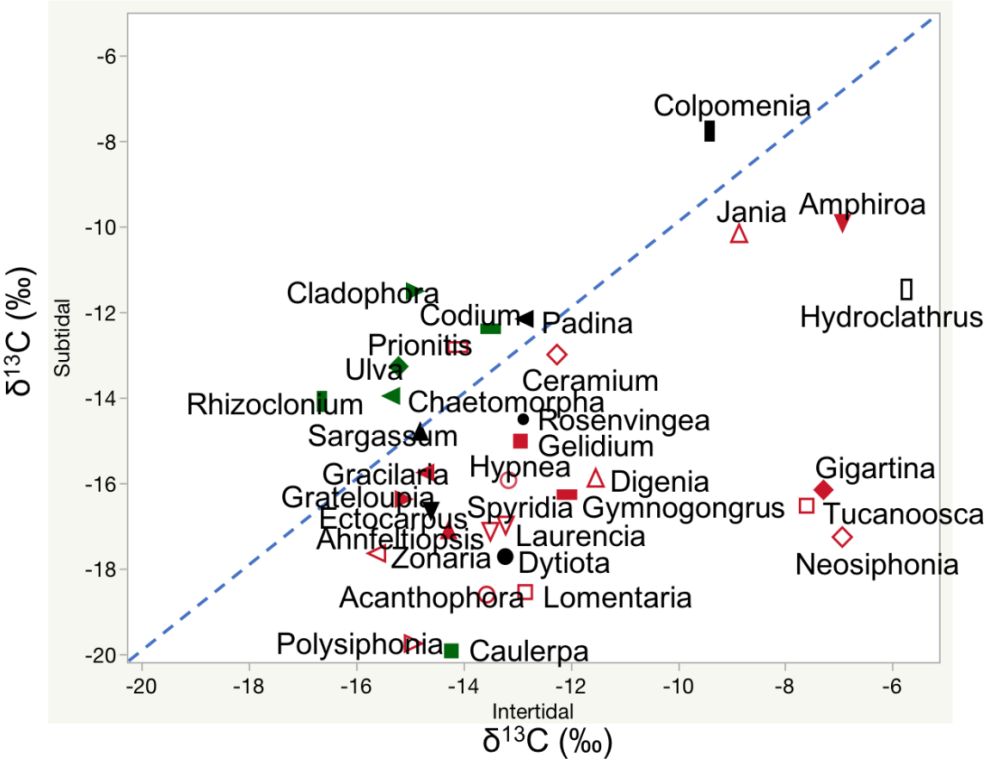


1042

1043 **Fig 4**

https://doi.org/10.5194/bg-2021-50
Preprint. Discussion started: 9 March 2021




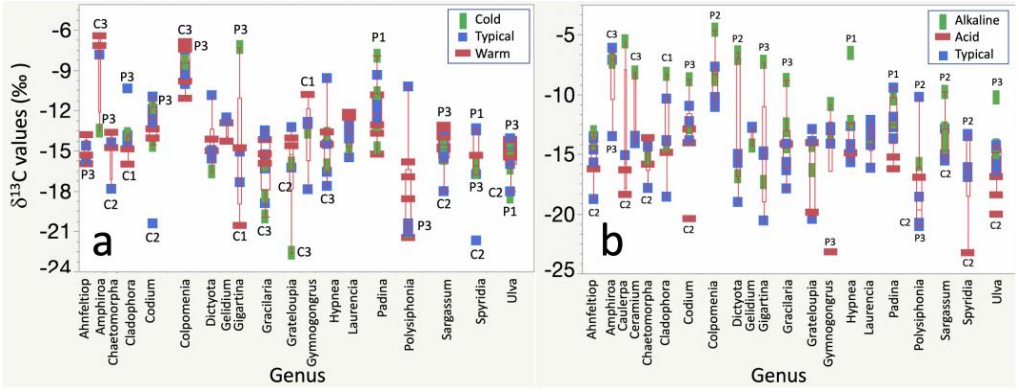


**Fig 5**

https://doi.org/10.5194/bg-2021-50
Preprint. Discussion started: 9 March 2021


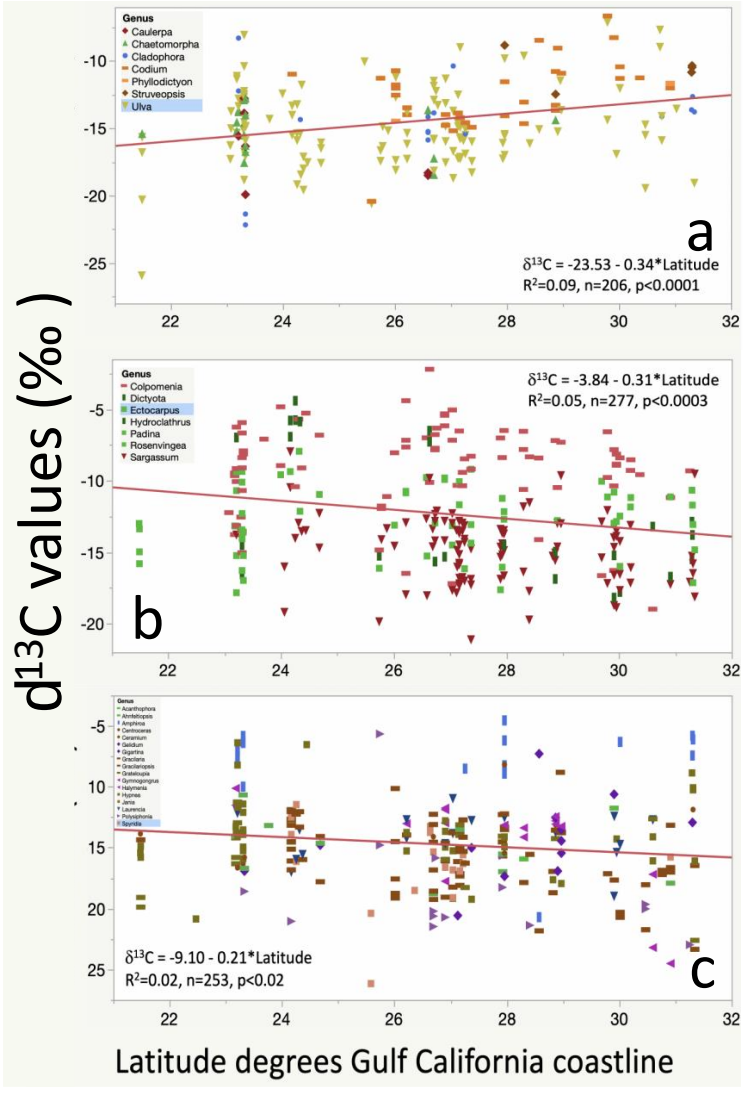


1046

1047 **Fig 6**

https://doi.org/10.5194/bg-2021-50
Preprint. Discussion started: 9 March 2021




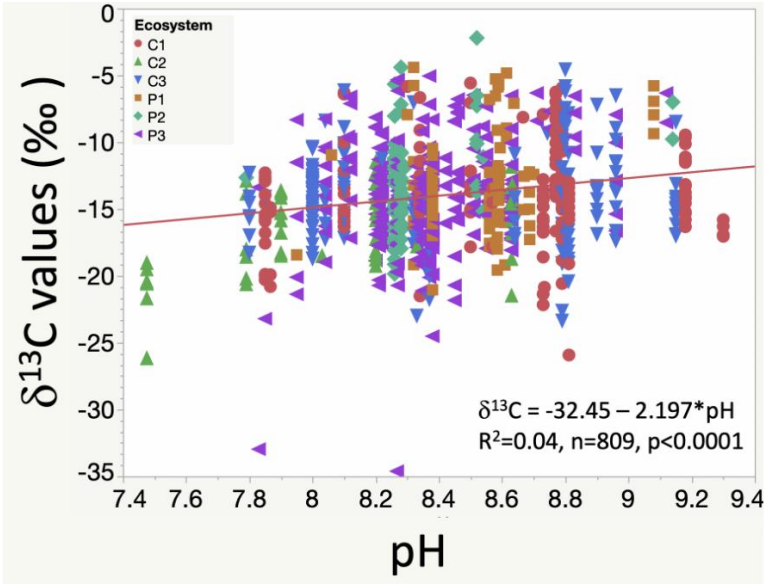


1048

1049 **Fig 7**

https://doi.org/10.5194/bg-2021-50
Preprint. Discussion started: 9 March 2021


Biogeosciences Discussions Open Access EGU

Table 1. Carbon isotopic composition (‰) in species of phyla Chlorophyta collected along Gulf of California coastlines.

| Species (n composite samples) | $\delta^{13}C \pm SD$ (Min to Max, ‰) |
|---|---|
| *Chaetomorpha* sp. (3) | -13.7±0.83 (-14.56 to -12.9) |
| *C. antennina* (10) | -14.58±1.10 (-16.29 to -12.79) |
| *C. linum* (5) | -16.84±1.65 (-18.45 to -14.6) |
| *Codium* sp. (5) | -11.6±3.01 (-14.07 to-6.65) |
| *C. amplivesiculatum* (8) | -14.44±2.74 (-20.42 to -11.25) |
| *C. brandegeei* (7) | -11.82±1.24 (-13.67 to -10.43) |
| *C. fragile* (4) | -13.0±2.66 (-14.78 to -9.04) |
| *C. simulans* (9) | -11.4±2.20 (-14.92 to -8.26) |
| *Ulva* sp. (12) | -13.98±3.85 (-19.16 to -7.11 |
| *U. acanthophora* (25) | -15.78±1.72 (-18.27 to -11.44) |
| *U. clathrata* (8) | -16.35± 2.01 (-20.54 to -14.52) |
| *U. compressa* (4) | -17.84±2.39 (-20.58 to -15.42) |
| *U. flexuosa* (13) | -16.03±3.67 (-25.92 to -10.38) |
| *U. intestinalis* (16) | -15.29±2.54 (-20.29 to -8.95) |
| *U. lactuca* (31) | -14.1±3.14 (-19.56 to -7.67) |
| *U. linza* (6) | -15.56±2.44 (-19.43 to -13.21) |
| *U. lobata* (5) | -13.18±1.87 (-15.33 to -11.11) |
| *U. prolifera* (3) | -14.24±1.76 (-15.49 to -12.22) |

1050

https://doi.org/10.5194/bg-2021-50
Preprint. Discussion started: 9 March 2021


Table 2. Carbon isotopic composition (‰) in species of phyla Ochrophyta collected along Gulf of California coastlines.

| Species (n composite samples) | $\delta^{13}C \pm SD$ (Min to Max, ‰) |
|---|---|
| *Colpomenia* sp. (11) | -10.97±3.65 (-18.98 to -5.42) |
| *C. ramosa* (4) | -11.43±2.55 (-13.76 to-7.81) |
| *C. sinuosa* (7) | -10.18±2.95 (-16.27 to -7.18) |
| *C. tuberculata* (64) | -8.72±3.20 (-19.19 to -2.20) |
| *Padina* sp. (15) | -11.1±1.53 (-13.06 to-7.94) |
| *P. crispata* (3) | -11.27±1.71 (-12.47 to -10.06) |
| *P. durvillaei* (36) | -13.2±2.59 (-19.97 to -9.19) |
| *Sargassum* sp. (34) | -14.25±2.36 (-18.71 to -7.95) |
| *S. herporhizum* (7) | -13.65±1.63 (-16.59 to -11.51) |
| *S. horridum* (12) | -15.52±2.89 (-19.72 to-9.52) |
| *S. johnstonii* (10) | -15.41±1.98 (-17.71 to -11.8) |
| *S. lapazeanum* (7) | -14.49±1.59 (-17.19 to -12.81) |
| *S. sinicola* (31) | -15.11±2.41 (-21.1 to -12.13) |

1051

https://doi.org/10.5194/bg-2021-50
Preprint. Discussion started: 9 March 2021




1052 Table 3. Carbon isotopic composition (‰) in species of phyla Rhodophyta collected along Gulf of
1053 California coastlines.

| Species (n composite samples) | $\delta^{13}C \pm SD$ (Min to Max, ‰) |
|---|---|
| *Gracilaria* sp. (18) | -15.48±2.43 (-21.83 to -12.24) |
| *Gracilaria* sp.2 (3) | -14.41±3.71 (-18.7 to -12.26) |
| *G. crispata* (7) | -15.07±2.96 (-19.13 to -10.14) |
| *G. pacifica* (6) | -16.48±1.64 (-18.57 to -13.61) |
| *G. spinigera* (3) | -14.94±3.84 (-17.66 to -12.23) |
| *G. subsecundata* (8) | -15.93±2.82 (-20.31 to -12.78) |
| *G. tepocensis* (3) | -15.1±1.92 (-17.01 to -13.16) |
| *G. textorii* (4) | -16.2±2.62 (-18.05 to -14.35) |
| *G. turgida* (5) | -15.34±3.56 (-20.72 to -12.04 |
| *G. vermiculophylla* (16) | -15.88±3.83 (-23.35 to -8.81) |
| *Hypnea* sp. (14) | -14.95±2.56 (-20.85 to -11.41) |
| *H. johnstonii* (5) | -11.18±3.52 (-13.76 to -6.54) |
| *H. pannosa* (5) | -11.8±3.31 (-14.95 to -6.39) |
| *H. spinella* (6) | -16.44±1.75 (-19.23 to -14.87) |
| *H. valentiae* (6) | -15.24±2.32 (-19.16 to -12.66) |
| *Laurencia* sp. (8) | -12.92±1.22 (-14.65 to -10.95) |
| *L. pacifica* (8) | -14.86±2.19 (-18.97 to -12.69) |
| *L. papillosa* (3) | -15.75±0.28 (-15.95 to -15.55) |
| *Spyrida* sp. (5) | -17.06±1.120 (-19.11 to -16.13) |
| *S. filamentosa* (14) | -15.86±3.83 (-26.16 to -11.46) |

1054

1055

1056

https://doi.org/10.5194/bg-2021-50
Preprint. Discussion started: 9 March 2021




1057 Table 4. Summary of the estimated regression coefficients for each simple linear regression
1058 analyses and on the constant of fitted regression models. Estimated regression coefficients includes
1059 degrees of freedom for the error (DFE), root-mean-square error (RMSE), coefficients of
1060 determination ($R^2$) and the adjusted $R^2$ statistics, Mallow's Cp criterion (Cp), Akaike Information
1061 Criterion (AIC), Bayesian Information Criterion (BIC) minimum, F Ratio test, and p-value for the
1062 test (Prob > F). Models information includes value of the constant a ($\delta^{13}C$, ‰), standard error (SE),
1063 t ratio and Prob > |t| (values * are significant).

| | Estimated regression coefficients | | | | | | | | | Model constant (a) | | | |
|---|---|---|---|---|---|---|---|---|---|---|---|---|---|
| Independent variables | DFE | RMSE | $R^2$ | Adjust $R^2$ | Cp | AICc | BIC | F ratio | Prob > F | $\delta^{13}C$ (‰) | SE | t ratio | Prob > \|t\| |
| Inherent macroalgae properties | | | | | | | | | | | | | |
| Phyla | 806 | 3.66 | 0.08 | 0.07 | 3 | 4,401 | 4,420 | 33.1 | <.0001** | -13.98 | 0.13 | -107.4 | <.0001** |
| Morphofunctional | 788 | 3.10 | 0.35 | 0.34 | 21 | 4,149 | 4,251 | 21.6 | <.0001** | -14.21 | 0.35 | -40.80 | <.0001** |
| Genero | 746 | 2.92 | 0.46 | 0.41 | 63 | 4,104 | 4,393 | 10.1 | <.0001** | -14.71 | 0.23 | -62.64 | <.0001* |
| Species | 641 | 2.79 | 0.57 | 0.46 | 168 | 4,195 | 4,898 | 5.2 | <.0001** | -14.60 | 0.16 | -93.22 | <.0001** |
| Biogeographical collection zone | | | | | | | | | | | | | |
| GC coastline | 807 | 3.79 | 0.01 | 0.01 | 2 | 4,456 | 4,470 | 7.4 | 0.0067* | -13.97 | 0.13 | -104.5 | <.0001** |
| Coastal sector | 803 | 3.73 | 0.05 | 0.04 | 6 | 4,433 | 4,465 | 7.9 | <.0001* | -14.12 | 0.16 | -90.85 | <.0001** |
| Latitude | 807 | 3.80 | 0.00 | 0.00 | 2 | 4,462 | 4,476 | 1.5 | 0.23 | -12.25 | 1.41 | -8.71 | <.0001** |
| Longitude | 807 | 3.81 | 0.00 | -0.00 | 2 | 4,463 | 4,477 | 0.1 | 0.80 | -15.44 | 5.83 | -2.65 | 0.0082* |
| Habitat features | | | | | | | | | | | | | |
| Substrate | 807 | 3.80 | 0.00 | 0.00 | 2 | 4,460 | 4,474 | 3.2 | 0.08 | -13.82 | 0.15 | -92.06 | <.0001* |
| Hydrodynamic | 807 | 3.80 | 0.00 | 0.00 | 2 | 4,462 | 4,476 | 1.3 | 0.26 | -13.88 | 0.15 | -95.00 | <.0001** |
| Emersion level | 807 | 3.69 | 0.06 | 0.06 | 2 | 4,412 | 4,427 | 52.2 | <.0001** | -14.05 | 0.13 | -107.6 | <.0001** |
| Environmental conditions | | | | | | | | | | | | | |
| Temperature | 802 | 3.70 | 0.01 | 0.01 | 2 | 4,390 | 4,404 | 5.4 | 0.0207* | -16.11 | 0.96 | -16.78 | <.0001* |
| pH | 807 | 3.73 | 0.04 | 0.04 | 2 | 4,430 | 4,444 | 33.4 | <.0001** | -32.45 | 3.21 | -10.13 | <.0001** |
| Salinity | 806 | 3.80 | 0.00 | -0.00 | 2 | 4,456 | 4,470 | 0.9 | 0.34 | -15.77 | 1.91 | -8.27 | <.0001** |

1064 *p<0.05, **p<0.0001

1065

1066

https://doi.org/10.5194/bg-2021-50
Preprint. Discussion started: 9 March 2021




1067 Table 5. Summary of the estimated regression coefficients for each multivariate linear
1068 regression analyses and on their constant of fitted regression models performed in
1069 individuals binned by genus. Estimated regression coefficients include degrees of freedom
1070 for the error (DFE), root-mean-square error (RMSE), coefficients of determination ($R^2$) and
1071 the adjusted $R^2$ statistics, Mallow's Cp criterion (Cp), Akaike Information Criterion (AIC),
1072 Bayesian Information Criterion (BIC) minimum, F Ratio test, and p-value for the test (Prob
1073 > F). Model information includes value of the constant a ($\delta^{13}C$, ‰), standard error (SE), t
1074 ratio and Prob > |t| (values * are significant).

| | Estimated regression coefficients | | | | | | | | | Model constant (a) | | | |
|---|---|---|---|---|---|---|---|---|---|---|---|---|---|
| Independent variables | DFE | RMSE | $R^2$ | Adjust $R^2$ | Cp | AICc | BIC | F ratio | Prob > F | $\delta^{13}C$ (‰) | SE | t ratio | Prob > \|t\| |
| Coastal sector | 652 | 2.78 | 0.57 | 0.47 | 157 | 4,169 | 4,834 | 20.0 | <.0001* | -17.52 | 0.64 | -27.24 | <.0001* |
| Substrate | 711 | 2.90 | 0.49 | 0.42 | 98 | 4,140 | 4,577 | 0.4 | 0.52 | -16.35 | 0.62 | -26.20 | <.0001* |
| Hydrodynamic | 714 | 2.87 | 0.50 | 0.43 | 95 | 4,120 | 4,545 | 0.1 | 0.78 | -16.53 | 0.64 | -25.95 | <.0001* |
| Emersion level | 713 | 2.77 | 0.53 | 0.47 | 96 | 4,060 | 4,489 | 153.0 | <.0001* | -16.65 | 0.60 | -27.85 | <.0001* |
| Temperature | 695 | 2.81 | 0.50 | 0.43 | 109 | 4,083 | 4,564 | 98.4 | <.0001* | -14.60 | 0.92 | -15.91 | <.0001* |
| Temperature ranges | 686 | 2.87 | 0.49 | 0.40 | 118 | 4,128 | 4,645 | 97.7 | <.0001* | -12.91 | 0.40 | -31.97 | <.0001* |
| pH | 701 | 2.86 | 0.51 | 0.43 | 108 | 4,134 | 4,611 | 156.6 | <.0001* | -28.57 | 2.69 | -10.64 | <.0001* |
| pH ranges | 697 | 2.67 | 0.57 | 0.51 | 112 | 4,028 | 4,522 | 152.2 | <.0001* | -16.39 | 0.58 | -28.05 | <.0001* |
| Salinity | 697 | 2.89 | 0.50 | 0.42 | 111 | 4,151 | 4,640 | 162.2 | <.0001* | -17.75 | 1.63 | -10.88 | <.0001* |
| Salinity ranges | 721 | 2.91 | 0.47 | 0.41 | 86 | 4,117 | 4,504 | 167.8 | <.0001* | -17.64 | 0.74 | -23.68 | <.0001* |

1075
1076
1077
1078
1079
1080

https://doi.org/10.5194/bg-2021-50
Preprint. Discussion started: 9 March 2021




1081 Table 6. Summary of the estimated regression coefficients for each multivariate linear regression
1082 analyses and on their constant of fitted regression models performed in individuals binned by
1083 coastline sector and genus. Estimated regression coefficients include degrees of freedom for the
1084 error (DFE), root-mean-square error (RMSE), coefficients of determination ($R^2$) and the adjusted
1085 $R^2$ statistics, Mallow's Cp criterion (Cp), Akaike Information Criterion (AIC), Bayesian
1086 Information Criterion (BIC) minimum, F Ratio test, and p-value for the test (Prob > F). Model
1087 information includes value of the constant a ($\delta^{13}C$, ‰), standard error (SE), t ratio and Prob > |t|
1088 (values * are significant).

| | Estimated regression coefficients | | | | | | | | | Model constant (a) | | | |
|---|---|---|---|---|---|---|---|---|---|---|---|---|---|
| Independent variables | DFE | RMSE | $R^2$ | Adjust $R^2$ | Cp | AICc | BIC | F ratio | Prob > F | $\delta^{13}C$ (‰) | SE | t ratio | Prob > \|t\| |
| Substrate | 590 | 2.76 | 0.62 | 0.47 | 219 | 4,287 | 5,155 | 15.8 | <.0001* | -17.08 | 0.66 | -25.72 | <.0001* |
| Hydrodynamic | 592 | 2.73 | 0.62 | 0.49 | 217 | 4,266 | 5,128 | 18.6 | <.0001* | -17.18 | 0.67 | -25.70 | <.0001* |
| Protection level | 590 | 2.75 | 0.62 | 0.48 | 219 | 4,285 | 5,153 | 20.0 | <.0001* | -17.51 | 0.64 | -27.22 | <.0001* |
| Emersion level | 603 | 2.69 | 0.63 | 0.50 | 206 | 4,217 | 5,045 | 18.6 | <.0001* | -17.47 | 0.64 | -27.49 | <.0001* |
| Temperature ranges | 569 | 2.74 | 0.61 | 0.46 | 235 | 4,293 | 5,202 | 28.0 | <.0001* | -13.73 | 0.45 | -30.32 | <.0001* |
| pH ranges | 580 | 2.50 | 0.69 | 0.57 | 229 | 4,155 | 5,051 | 9.7 | 0.0019* | -16.88 | 0.62 | -27.15 | <.0001* |
| Salinity ranges | 631 | 2.76 | 0.58 | 0.47 | 176 | 4,183 | 4,913 | 21.2 | <.0001* | -18.30 | 0.79 | -23.05 | <.0001* |

1089

1090

https://doi.org/10.5194/bg-2021-50
Preprint. Discussion started: 9 March 2021




1091 Table 7. Summary of the estimated regression coefficients for each multivariate linear regression
1092 analyses and on their constant of fitted regression models performed in individuals binned in
1093 coastline sector, habitats features, environmental conditions, and Physiological performed
1094 separately by morpho-functional groups and genus. Estimated regression coefficients include
1095 degrees of freedom for the error (DFE), root-mean-square error (RMSE), coefficients of
1096 determination ($R^2$) and the adjusted $R^2$ statistics, Mallow's Cp criterion (Cp), Akaike Information
1097 Criterion (AIC), Bayesian Information Criterion (BIC) minimum, F Ratio test, and p-value for the
1098 test (Prob > F). Model information includes value of the constant a ($\delta^{13}C$, ‰), standard error (SE),
1099 t ratio and Prob > |t| (values * are significant).

| | | | Estimated regression coefficients | | | | | | | Model constant (a) | | | |
|---|---|---|---|---|---|---|---|---|---|---|---|---|---|
| Full model | DFE | RMSE | $R^2$ | Adjust $R^2$ | Cp | AICc | BIC | F ratio | Prob > F | $\delta^{13}C$ (‰) | SE | t ratio | Prob > \|t\| |
| Coastline sector + Habitats features + Morphofunctional group | | | | | | | | | | | | | |
| I-Morpho-functional | 593 | 2.79 | 0.60 | 0.46 | 216 | 4,301 | 5,160 | 20.8 | <.0001* | -13.49 | 0.57 | -23.52 | <.0001* |
| Coastline sector + Environmental conditions + Morphofunctional group | | | | | | | | | | | | | |
| II-Morpho-functional | 680 | 2.90 | 0.51 | 0.42 | 129 | 4,189 | 4,750 | 25.1 | <.0001* | -13.42 | 0.54 | -24.74 | <.0001* |
| Coastline sector + Habitat features+ Genus | | | | | | | | | | | | | |
| I-Genus | 482 | 2.66 | 0.71 | 0.51 | 327 | 4,565 | 5,655 | 15.8 | <.0001* | -16.93 | 0.73 | -23.27 | <.0001* |
| Coastline sector + Environmental conditions + Genus | | | | | | | | | | | | | |
| II-Genus | 494 | 2.49 | 0.72 | 0.55 | 310 | 4,374 | 5,438 | 14.8 | 0.0001* | -13.55 | 0.64 | -21.17 | <.0001* |

1100

https://doi.org/10.5194/bg-2021-50
Preprint. Discussion started: 9 March 2021


1101 Table 8. Constant of fitted regression model explaining the $\delta^{13}C$ variability by morpho-functional
1102 groups. Model information includes value of the constant a ($\delta^{13}C$, ‰), standard error (SE), t ratio
1103 and Prob > |t|. Only morpho-functional groups with significant effects are enlisted.

| Term | Estimated | SE | Razón t | Prob > \|t\| |
|---|---|---|---|---|
| Model constant | -14.21 | 0.35 | -40.80 | <.0001** |
| R-Smaller-sized articulated corallines | 4.48 | 1.74 | 2.58 | 0.0100* |
| O-Compressed with branched or divided thallus | 1.24 | 0.46 | 2.66 | 0.0079* |
| C-Erect thallus | 1.76 | 0.62 | 2.84 | 0.0046* |
| R-Larger-sized articulated corallines | 6.32 | 0.80 | 7.95 | <.0001* |
| O-Hollow with spherical or subspherical shape | 4.96 | 0.47 | 10.51 | <.0001* |
| R-Blade-like with one of few layers of cells | -5.89 | 2.97 | -1.98 | 0.0476* |
| C-Tubular | -1.62 | 0.50 | -3.26 | 0.0012** |
| R-Filamentous uni&pluriseriate with erect thallus | -2.15 | 0.55 | -3.92 | <.0001* |
| R-Flattened macrophytes with cortication | -8.89 | 1.25 | -7.10 | <.0001* |

1104 *p<0.05, **p<0.0001
1105
1106
1107
1108
1109
1110
1111
1112

https://doi.org/10.5194/bg-2021-50
Preprint. Discussion started: 9 March 2021




1113 Table 9. Constant of fitted regression model explaining the $\delta^{13}C$ variability by genus. Model
1114 information includes value of the constant a ($\delta^{13}C$, ‰), standard error (SE), t ratio and Prob > |t|.
1115 Only genus with significant effects are enlisted.

| Term | Estimated | SE | Razón t | Prob > \|t\| |
|---|---|---|---|---|
| Model constant | -14.70 | 0.23 | -62.64 | <.0001** |
| *Corallina* | 6.40 | 2.88 | 2.22 | 0.0269* |
| *Tacanoosca* | 3.54 | 1.31 | 2.71 | 0.0070* |
| *Jania* | 4.98 | 1.68 | 2.97 | 0.0031* |
| *Struveopsis* | 4.12 | 1.31 | 3.15 | 0.0017* |
| *Codium* | 2.26 | 0.55 | 4.08 | <.0001** |
| *Padina* | 2.19 | 0.46 | 4.8 | <.0001** |
| *Hydroclathrus* | 7.33 | 1.11 | 6.59 | <.0001** |
| *Amphiroa* | 6.84 | 0.76 | 9.05 | <.0001** |
| *Colpomenia* | 5.45 | 0.39 | 14.02 | <.0001* |
| *Spyridia* | -1.46 | 0.70 | -2.10 | 0.0361* |
| Gracilaria | -0.89 | 0.41 | -2.18 | 0.0294* |
| Polysiphonia | -3.75 | 0.78 | -4.82 | <.0001** |
| Schizymenia | -19.08 | 2.05 | -9.33 | <.0001** |

1116 *p<0.05, **p<0.001
1117
1118

https://doi.org/10.5194/bg-2021-50
Preprint. Discussion started: 9 March 2021


Biogeosciences Discussions Open Access EGU

1119 Table 10. Constant of fitted regression model explaining the $\delta^{13}C$ variability by species. Model
1120 information includes value of the constant a ($\delta^{13}C$, ‰), standard error (SE), t ratio and Prob > |t|.
1121 Only genus with significant effects are enlisted.

| Term | $\delta^{13}C$, ‰ estimated | SE | Razón t | Prob > \|t\| |
|---|---|---|---|---|
| Constante del modelo | -14.59 | 0.16 | -93.22 | <.0001** |
| *Hypnea pannosa* | 2.79 | 1.25 | 2.24 | 0.0256* |
| *Colpomenia ramosa* | 3.16 | 1.39 | 2.27 | 0.0237* |
| *Corallina vancouverensis* | 6.29 | 2.78 | 2.27 | 0.0238* |
| *Caulerpa peltata* | 3.86 | 1.61 | 2.4 | 0.0165* |
| *Codium* sp. | 3.00 | 1.25 | 2.4 | 0.0167* |
| *Amphiroa misakiensis* | 7.08 | 2.78 | 2.55 | 0.0110* |
| *Jania* sp. | 5.04 | 1.97 | 2.56 | 0.0106* |
| *Codium brandegeei* | 2.78 | 1.06 | 2.63 | 0.0088** |
| *Hypnea johnstonii* | 3.42 | 1.25 | 2.74 | 0.0063** |
| *Tacanoosca uncinata* | 3.43 | 1.25 | 2.74 | 0.0062** |
| *Struveopsis* sp. | 3.98 | 1.39 | 2.86 | 0.0044** |
| *Padina durvillaei* | 1.40 | 0.49 | 2.87 | 0.0043** |
| *Amphiroa* sp.*3* | 8.20 | 2.78 | 2.95 | 0.0033** |
| *Codium simulans* | 3.19 | 0.94 | 3.41 | 0.0007** |
| *Amphiroa* sp.2 | 6.59 | 1.61 | 4.1 | <.0001** |
| *Colpomenia sinuosa* | 4.42 | 1.06 | 4.17 | <.0001** |

https://doi.org/10.5194/bg-2021-50
Preprint. Discussion started: 9 March 2021




| | | | | |
|---|---|---|---|---|
| *Colpomenia* sp. | 3.63 | 0.85 | 4.27 | <.0001** |
| *Padina* sp. | 3.50 | 0.73 | 4.77 | <.0001** |
| *Hydroclathrus clathratus* | 7.22 | 1.06 | 6.82 | <.0001** |
| *Amphiroa* sp. | 8.12 | 0.94 | 8.67 | <.0001** |
| *Colpomenia tuberculata* | 5.87 | 0.38 | 15.45 | <.0001** |
| *Spyrida* sp. | -2.46 | 1.25 | -1.97 | 0.0496* |
| *Pyropia thuretii* | -5.50 | 2.78 | -1.98 | 0.0480* |
| *Ulva acanthophora* | -1.19 | 0.58 | -2.06 | 0.0399* |
| *Grateloupia filicina* | -2.37 | 1.14 | -2.08 | 0.0382* |
| *Rhodymenia* sp. | -4.08 | 1.97 | -2.08 | 0.0380* |
| *Ulva compressa* | -3.24 | 1.39 | -2.33 | 0.0203* |
| *Rhizoclonium riparium* | -5.06 | 1.61 | -3.15 | 0.0017** |
| *Polysiphonia* sp. | -4.81 | 1.39 | -3.44 | 0.0006** |
| *Halymenia actinophysa* | -9.91 | 2.78 | -3.57 | 0.0004** |
| *Cladophora microcladioides* | -7.16 | 1.97 | -3.64 | 0.0003** |
| *Polysiphonia mollis* | -5.22 | 1.06 | -4.93 | <.0001** |
| *Schizymenia pacifica* | -19.19 | 1.97 | -9.76 | <.0001** |

*p<0.05, **p<0.001